European Commission

JRC SCIENTIFIC AND POLICY REPORTS

Total and radiative capture cross section measurements for ^{238}U at GELINA and n_TOF

Deliverable for the ANDES project

P. Schillebeeckx, C. Lampoudis, F. Mingrone T. Wright, B. Becker, E. Berthoumieux, J. Billowes, D. Cano-Ott, R. Dagan, J.C. Drohe, C. Guerrero, F. Gunsing, S. Kopecky, C. Massimi, E. Mendoza, G. Vannini, R. Wynants and the n_TOF collaboration

2013

Report EUR 26478 EN

Joint Research Centre

European Commission
Joint Research Centre
Institute for Reference Materials and Measurements

Contact information
Peter Schillebeeckx
Address: Joint Research Centre, Retieseweg 111, B-2440 Geel, Belgium
E-mail: peter.schillebeeckx@ec.europa.eu
Tel.: +32 14 57 1475
Fax: +32 14 57 1862

http://irmm.jrc.ec.europa.eu/
http://www.jrc.ec.europa.eu/

JRC87402

EUR 26478 EN

ISBN 978-92-79-35279-9 (pdf)

ISSN 1831-9424 (online)

doi:10.2787/86726

Luxembourg: Publications Office of the European Union, 2013

Printed in Belgium

Total and radiative capture cross section measurements for ^{238}U at GELINA and n_TOF

The ANDES deliverable 1.8 of Work Package 1, Task 1.2

P. Schillebeeckx[1], C. Lampoudis[1], F. Mingrone[2], T. Wright[3], B. Becker[1], E. Berthoumieux[4,5], J. Billowes[3], D. Cano Ott[6], R. Dagan[7], J.C. Drohe[1], C. Guerrero[5], F. Gunsing[4], S. Kopecky[1], C. Massimi[2], E. Mendoza[6], G. Vannini[2], R. Wynants[1] and the n_TOF collaboration[8]

[1]European Commission, Joint Research Centre, Institute for Reference Materials and Measurements, Retieseweg 111, B - 2440 Geel, Belgium

[2]Dipartimento di Fisica, Università di Bologna, and Sezione INFN di Bologna, I-40126, Italy

[3]School of Physics and Astronomy, University of Manchester, Oxford Road, Manchester, UK

[4]CEA-Saclay, Irfu/SPhN, F-91191 Gif-sur-Yvette, France

[5]CERN, Geneva (CH)

[6]CIEMAT, Nuclear Innovation Unit, Madrid (ES)

[7]Karlsruhe Institute of Technology, INR, 76344, Eggenstein-Leopoldshafen, Germany

[8]www.cern.ch/ntof

31 October 2013

Contents

1. Introduction

According to the Description of Work of the ANDES project, Work Package 1 (WP1) "Measurement for Advanced Reactor Systems" consists of four tasks [1]. This document reports on the deliverable D1.8 of Task 1.2 of WP1. Task 1.2 is entitled "High accuracy measurements of neutron capture cross sections" and is aimed at improving the cross sections for neutron induced capture reactions on ^{238}U, ^{241}Am and the main Cm isotopes. These objectives are pursued through five sub-tasks. The deliverable D1.8 reports on total and radiative neutron capture cross section measurements for ^{238}U at the time-of-flight facilities GELINA and n_TOF and summarizes the activities of subtask 1.2.a and 1.2.c:

Subtask 1.2.a: "^{238}U total and radiative neutron capture measurements at JRC"
Total and capture cross section measurements will be performed at the GELINA facility of the EC-JRC-IRMM applying the time-of-flight technique and transmission factors and capture yields will be determined. Resonance shape analysis to deduce resonance parameters and statistical nuclear reaction analysis to deduce average resonance parameters and average cross sections will be employed.

Subtask 1.2.c: "^{238}U radiative neutron capture measurements at CERN n_TOF"
Capture cross section measurements will be performed at n_TOF with two different arrangements: C_6D_6 total energy detectors and the n_TOF total absorption detector. Capture yields will be deduced and resonance shape analysis will be performed to deduce resonance parameters in the resolved resonance region, while statistical nuclear reaction models will be applied to deduce average resonance parameters and average cross sections in the unresolved resonance region.

These subtasks were executed in close collaboration between various institutes, in particular CEA Saclay (FR), CIEMAT (ES), EC-JRC-IRMM, INFN Bologna (IT) and the University of Manchester (UK) and CERN (CH). This report summarizes the work performed, the achievements made and perspectives for future use of the data. In addition, a list of published papers and conference contributions that served to disseminate the activities of the ANDES project is given. The report provides evidence of a successful completion of subtasks 1.2.a and 1.2.c. The outcome provides important experimental data to improve the nuclear data of ^{238}U in the main nuclear libraries. More in particular, the results of these subtasks will be an important input to the CIELO (Collaborative International Evaluated Library Organization) project, which is a new working paradigm to facilitate evaluated nuclear reaction data advances [2].

2. Motivation and objectives

The cross section for the neutron induced capture reaction on ^{238}U is an important quantity for the design and safe operation of nuclear reactors. The capture cross section in the unresolved resonance region is of special importance for innovative reactor systems. Despite the importance of this cross section, inconsistencies between experimental data published in the literature may reach 15%. Therefore, the capture cross section for ^{238}U in both the resolved (RRR) and unresolved (URR) resonance region is on the Nuclear Data High Priority Request List [3]. This list represents a compilation of the most important nuclear data requirements and is maintained by the Nuclear Energy Agency of the OECD. The cross section between 22 eV and 25 keV is requested with an uncertainty between 1% and 2%. Such an accuracy level is difficult to be obtained from results of a single measurement. In this context, complementary experiments at the GELINA [4] and n_TOF facility [5,6] were scheduled within task 1.2 of the ANDES project.

Experimental data for the capture cross section of ^{238}U in the resonance region can be obtained by applying the total energy detection or total γ–ray absorption principle [7]. To apply the total energy detection principle γ–ray detectors with a relatively low detection efficiency that is directly proportional to the γ–ray energy are required. Mostly C_6D_6 detectors are used in combination with the pulse height weighting technique [7-9]. An ideal detector for the total γ-ray absorption technique has a 4π geometry and a 100% absolute detection efficiency [7], like the total absorption detector installed at n_TOF [10]. Hence, these two principles are strongly different and have their advantages and disadvantages.

Combining results from two different detectors and independent measurement principles should result in a reduction of uncertainties due to systematic effects. Therefore, an experimental program was established based on measurements with C_6D_6 detectors at GELINA [4] and measurements with a similar C_6D_6 detection system [5] and a total γ-ray absorption detector at n_TOF [6]. In addition, the results of these capture cross section measurements will be complemented with data resulting from transmission measurements at GELINA. The final

objective is to provide capture cross section data which can be used for a new evaluation of the capture cross section of ^{238}U. The target uncertainty of the experimental data is less than 2% for the correlated component due to systematic effects such as the normalization and less than 2% for the uncorrelated component due to counting statistics. A similar approach has been followed to improve the status of the cross section for ^{241}Am(n,γ) [11].

3. Measurements at the GELINA facility of the EC-JRC-IRMM

GELINA is a multi-user, multi-purpose facility built for high-resolution neutron spectroscopy [12]. It provides a pulsed white neutron source with neutron energies ranging from 10 meV to 20 MeV. It uses a linear accelerator which produces a pulsed electron beam with a maximum energy of 150 MeV, a repetition rate between 50 Hz and 800 Hz and a 12 A peak current. A magnet is used to compress the pulsed electron beam to about 1 ns [13] before the electrons are stopped in a mercury-cooled rotating uranium target and Bremsstrahlung is generated [14]. Subsequently, neutrons are produced by photonuclear reactions. To produce a white neutron spectrum from thermal energy up to a few MeV, two 4-cm thick beryllium containers filled with water, are placed beneath and above the target as moderators. By shielding either the target or the moderator, the direct or moderated spectrum can be used. The total neutron intensity is monitored by two BF_3 proportional counters located in the concrete ceiling of the target hall. The intensity resulting from the response of these monitors is independent of the filter and/or sample configuration of the measurement stations. For the measurements discussed in this work the moderated spectrum was used and the accelerator was operated at a 800 Hz operating frequency. Both the transmission and capture experiments were carried out following the procedures described in Ref. [7].

In order to apply the time-of-flight (TOF) technique, 10 flight-paths are installed in a star-like configuration around the neutron production target. The flight tubes are under vacuum, they have a diameter of 50 cm and their lengths range up to 400 m. Several measurement stations are installed at different distances (with nominal distances of 10, 30, 50, 60, 100, 200, 300 and 400 m) along the flight paths. These experimental stations are equipped with a wide variety of detectors, and data acquisition systems. There are measurement set-ups for transmission experiments, capture, fission, elastic and inelastic cross sections, and flux measurements.

The processing of the time and amplitude signals for both the transmission and capture detection systems used for this work was based on analog electronics. Each system produced a veto signal that created a fixed dead time as soon as a time signal was produced. This fixed dead time was determined accurately by a measurement of the time-interval distribution of successive events. The dead time corrections for such a system are well understood as demonstrated in Ref. [7,15]. The maximum dead time correction hardly exceeded 10%, therefore the induced uncertainties are negligible. An in-house built fast-timing digitizer with a time resolution of 1.0 ns was used to determine the neutron time of flight. For all systems the amplitude and the time of flight of each event were recorded in list-mode for off-line data analysis. Each measurement was subdivided in different cycles. Only cycles for which the operating frequency, the total neutron production and the total response of the detection chain deviated from each other by less than 2.5% were selected.

To derive the experimental observables, i.e. experimental transmissions and reaction yields, from the TOF-histograms the AGS (Analysis of Geel Spectra) code as used [16]. The code, which has been developed at the EC-JRC-IRMM, is based on a compact formalism to propagate all uncertainties starting from uncorrelated uncertainties due to counting statistics. It stores the full covariance information after each operation in a concise, vectorized way. The AGS formalism results in a substantial reduction of data storage volume and provides a convenient structure to verify the various sources of uncertainties through each step of the data reduction process. The concept applied in AGS has been recommended by the Nuclear Data Section of the IAEA to store TOF observables in the EXFOR data base [17].

3.1 Transmission experiments

3.1.1 Experimental conditions

An extensive set of transmission data are available in the literature to evaluate the total cross section for neutron induced reactions on ^{238}U. They result mainly from high resolution measurements at the ORELA facility using different flight path distances (42 m, 150 m and 200 m) and samples with different thicknesses (0.0002 at/b to 0.175 at/b) [18-23]. In addition transmission measurements have been carried out at a 26.5-m station at GELINA by Meister et al. [24] using samples at 23.7 and 293.7 K. An example of the quality of these data is shown in Fig.1. In this figure the experimental transmissions derived by Olsen et al. [18] for the 1.85 10^{-4} at/b, 6.19 10^{-4} at/b and 12.4 10^{-4} at/b samples are compared with the theoretical transmission using the resonance

parameters resulting from an evaluation performed by Derrien et al. [25]. The results of this evaluation were adopted in the main nuclear libraries, i.e. ENDF/B-VII.1, JEFF 3.1.2, JENDL 4.0.

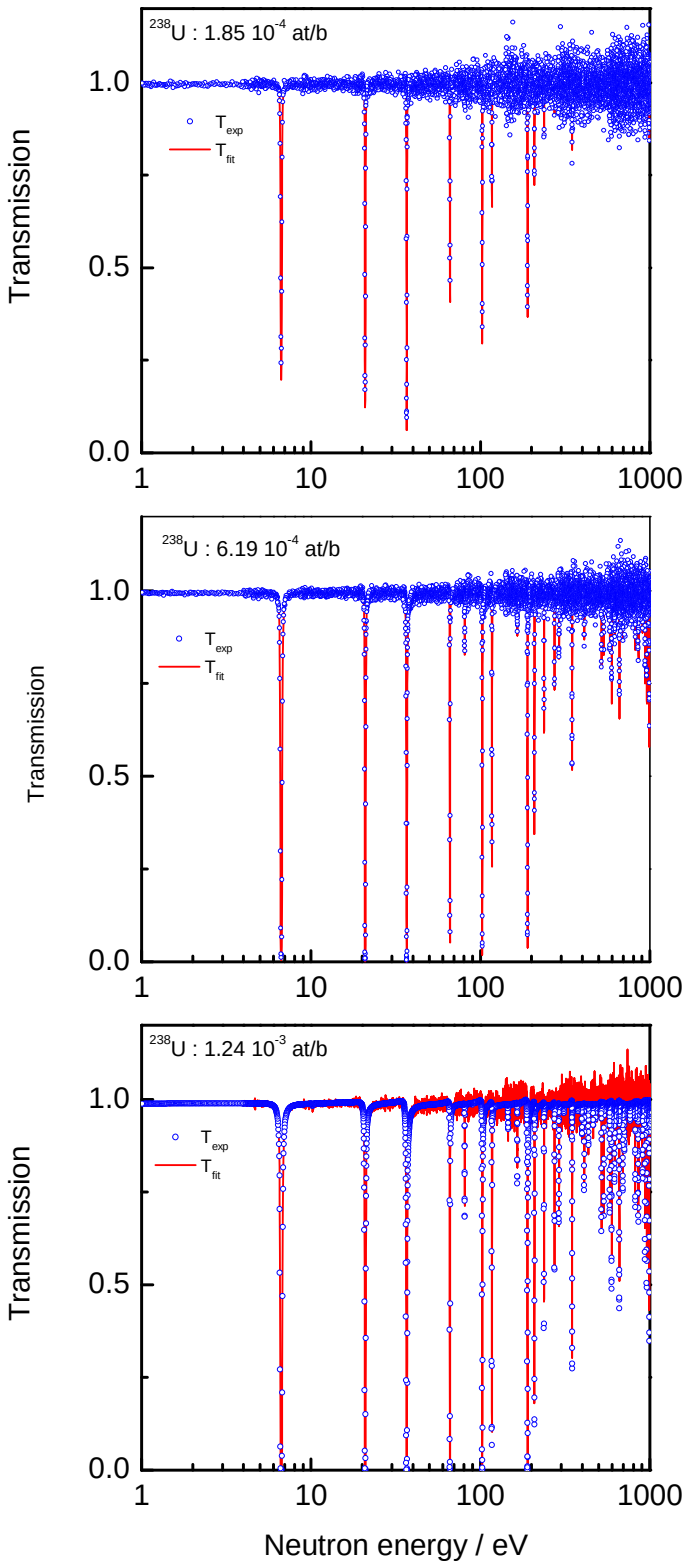

Fig.1 Comparison of the experimental transmission obtained by Olsen et al. [18] and the calculated transmission using the parameters of Derrien et al. [25].

Given the availability of these transmission data, only one transmission measurements was carried out at GELINA. This measurement was performed to verify the resonance energies and neutron widths of Derrien etal. [25]. A verification of the resonance energies is important since they were used to calibrate the flight path lengths of the capture and transmission stations of GELINA [26,27]. The transmission experiments were carried out at a 50 m measurement station of GELINA using a natural uranium metallic sample, with an areal density of 2.4 x 10^{-3} at/b. The flight path forms an angle of 9^{o} with the normal of the facet of the moderator viewing the flight path. The sample and detector were placed in a climatised room to keep them at a constant temperature of 22 ^{o}C.

3.1.2 Data reduction

The experimental transmission T_{exp} was obtained from the ratio of the counts of a sample-in measurement C_{in} and a sample-out measurement C_{out}, both corrected for their background contribution B_{in} and B_{out}, respectively [7]:

$$T_{exp} = N_T \frac{C_{in} - k_T\, B_{in}}{C_{out} - k_T\, B_{out}}. \qquad (1)$$

The TOF-spectra in Eq. 1 were corrected for losses due to the dead time in the detector and the electronics chain and all spectra were normalized to the same TOF-bin width and neutron intensity. The latter was derived from the response of the BF_3 beam monitors. The normalization factor N_T = 1.0000 ± 0.0025 was introduced to account for the uncertainty due to the normalization of the beam intensity. The background as a function of TOF was determined by an analytical expression applying the black resonance technique [7]. As discussed in Ref. [7], the best accuracy is obtained when measurements are carried out with fixed background filters. Using fixed filters, the impact of the sample or filter on the background level can be verified and the stability of the background level can be controlled. The factor k_T = 1.00 ± 0.03 introduces a correlated uncertainty component accounting for systematic effects due to the background model.

The zero point of the time scale was deduced from the position of the γ-ray flash with an uncertainty of 1 ns. The flight path length of the transmission station was calibrated using the (6.673 ± 0.001) eV resonance of ^{238}U determined by Derrien et al. [25]. These measurements were performed with a 100 Hz operating frequency of the accelerator.

3.2 Capture experiments

3.2.1 Experimental conditions

The capture measurements were carried out at a 12.5 m measurement station of flight path 5, which forms an angle of 18 degrees with respect to the normal of the moderator facet viewing the flight path. More details about this flight path station can be found in Ref. [28].

Two rectangular and almost identical metallic samples were mounted on a back-to-back configuration, resulting in a total uranium mass of 12.2 g and a combined thickness of 4.56 mm. The characteristics of the two samples are summarized in Table 1. Both samples originated from the same batch of uranium that was highly enriched in ^{238}U (99.99%). The isotopic composition of this batch was verified by mass spectrometry in 1984 and resulted in: ^{234}U < 1 ppm, ^{235}U 11 ppm and ^{236}U < 1 ppm. The areal density of the two samples was derived from a measurement of the mass and the area. The uncertainty on the areal density is 0.5%. The area was determined by an optical surface inspection with a microscopic based measurement system from Mitutoyo. The mass of the sample was determined before and after the measurement. The uncertainty on the areal density is mainly due to the uranium mass of the sample which changes during the measurement due to oxidation.

Table 1 Characteristics of the ^{238}U samples used in the capture measurements at GELINA.

Sample	Size mm x mm	Mass g	Areal density at/b
^{238}U (1)	53.67 x 30.21	6.170 ± 0.020	(9.570 ± 0.050) 10^{-4}
^{238}U (2)	53.08 x 30.03	6.030 ± 0.020	(9.628 ± 0.050) 10^{-4}

Apart from measurements with the uranium sample, the experimental campaign included additional runs using ^{nat}Ag, ^{nat}Pb and ^{208}Pb samples and only the sample holder. The ^{nat}Ag and ^{nat}Pb samples were samples with similar dimensions as the combined ^{238}U samples. The ^{nat}Ag sample was measured to verify the normalization.

The measurement with only the sample holder and the Pb-samples were carried out to determine the background contribution in the response of the C_6D_6 detectors. Fixed Na and S black resonance filters were used to continuously monitor the background at 2.85 keV and 102 keV and to account for the sample dependence of the background. Due to the presence of the S-filter, no additional filter was needed to reduce the intensity of the γ-ray flash.

Prompt γ-rays originating from neutron induced capture events were detected by two C_6D_6 liquid scintillators. The detectors form an angle of 125° with respect to the direction of the neutron beam to reduce effects caused by the anisotropy of the dipole radiation. The discrimination level of the capture detection system corresponded to 200 keV deposited energy. The total energy detection principle combined with the pulse height weighting technique was applied to make the detection efficiency for a capture event directly proportional to the total γ-ray energy available in the capture event. To transfer the light output of the scintillators, recorded in channels, into an electron equivalent light output, expressed in energy units, calibration measurements with radionuclide γ-ray sources (^{137}Cs (661 keV), ^{60}Co (1173 keV and 1332 keV), ^{232}Th (2.6 MeV), AmBe (4431 keV) and PuC (6130 keV)) were carried out. The stability of the C_6D_6 detectors was monitored twice a week by measurements of the 2.6 MeV γ-ray from the ^{232}Th decay chain.

The energy dependence of the neutron flux was measured in parallel with the prompt γ-rays based on the ^{10}B(n,α) neutron cross section standard [29], using a Frisch-gridded ionization chamber placed at about 80 cm distance before the sample. The impact of kinematic effects was strongly reduced by using two chambers with a common cathode loaded with two layers of ^{10}B. This back-to-back configuration, together with a bias on the amplitude spectrum that accepts the signal from both the ^{7}Li and α particle, rules out a systematic bias effect related to the forward-to-backward emission ratio [7].

Two sets of measurements with different collimation conditions of the neutron beam at the sample position, i.e. 80 and 70 cm diameter, were performed. This was done to reduce systematic effects due to the collimation of the neutron beam. The temperature inside the experimental station was controlled to keep the sample at a constant temperature of 22 °C and to minimize drifts in the detector chain. The accelerator was operated at a frequency of 800 Hz, with additional runs of 400 Hz to control the normalization using low energy resonances and to verify the contribution of overlap neutrons to the background. The measurements at 400 Hz and 800 Hz were carried out with a ^{nat}Cd (1mm thick) and ^{10}B (4.2 10^{-3} at/b) overlap filter, respectively. Measurements with S, Na, Co, W and Ag black resonance filters were used to determine the background of the neutron flux by the black resonance technique [7] and to verify the background correction applied for the C_6D_6 system. A fixed S and Na background filter were used. The use of this filter excludes the use of data around 102 and 2.9 keV. However, as discussed in Ref. [7] it improves the accuracy of the data in the URR.

3.2.2 Data reduction

The list mode data were sorted into TOF-histograms after verification of the stability of the detection systems. Each event recorded in the C_6D_6 detectors was weighted using a weighting function which was determined by Monte Carlo simulations as described in Ref. [8]. In the calculation of the weighting function the effect of the discrimination level was taken into account. To account for neutron and γ-ray transport in the sample the procedure described in Ref. [7, 8] was applied. The γ-rays were assumed to be homogeneously distributed in the sample and a correction factor, depending on the areal density and the total cross section, is applied when the resonance shape analysis is carried out.

The experimental yield Y_{exp} was derived from the ratio of the observed response of the capture detection system and the response of the neutron flux detector [7]:

$$Y_{exp} = \frac{N_c}{S_n + E_n \frac{A}{1+A}} \frac{C_w - B_w}{C_\varphi - B_\varphi} \frac{Y_\varphi}{T_\varphi}. \qquad (2)$$

The dead time corrected weighted response of the C_6D_6 detection system is denoted by C_w and its background contribution by B_w. The dead time corrected TOF spectrum resulting from the flux measurements is C_φ and its background contribution is B_φ. All spectra are normalized to the same neutron intensity. The quantity Y_φ/T_φ , dependent equivalently on TOF or energy, is given by:

$$\frac{Y_\varphi}{T_\varphi} = e^{n\sigma_{tot}} (1 - e^{-n\sigma_{tot}}) \frac{\sigma_\alpha}{\sigma_{tot}} \quad , \qquad (3)$$

where σ_{tot} and σ_{α} are the ^{10}B(n,tot) and ^{10}B(n,α) cross sections, respectively, and n is the total areal density of the two ^{10}B layers. The normalization factor N_c accounts for various effects, such as the effective beam-sample intersection factor, the solid angle between the sample and the detection system, the absolute detection efficiency and the absolute neutron flux.
The background for capture measurements consists of three contributions [7]: (1) a time independent component due to ambient radiation and possible long lived radioactivity in the sample and its surroundings; (2) a time dependent component independent of the sample and (3) a time dependent component depending on the sample characteristics. The first component can be estimated with a good accuracy from measurements just after the accelerator is switched off, or in a TOF region where the neutron flux is negligible. The time dependent component independent of sample properties can be deduced from measurements without a sample in the beam. The last component is the most difficult one to quantify. This component depends on the neutron and γ-ray scattering properties of the sample, on the neutron sensitivity of the detection system and on the characteristics of the measurement station. The neutron sensitivity in this discussion is the detector response due to neutrons which are scattered from the sample and create a capture reaction in the sample-detector environment. One has to differentiate between a direct and a delayed component. The direct component originates from scattered neutrons which cause an immediate capture reaction in the detector assembly. This contribution follows the resonance structure of the cross section and is hard to distinguish from the response due to a (n,γ) reaction in the sample. The delayed component is due to neutrons that scatter from the sample, enter the construction material of the measurement station or detector, where they slowdown before they create a capture reaction in the detector.

For the C_6D_6 detection system at GELINA the sample dependent background due to both the scattered γ-rays and the delayed component of the scattered neutrons can be neglected [7,28]. The background contribution to the weighted response can be approximated by [7]:

$$B_w(t_m) = b_0 + k_1\, C_{w,0}(t_m) + k_2\, R_n(t_m)(C_{w,Pb}(t_m) - C_{w,0}(t_m)) \quad , \qquad (4)$$

where b_o is a time independent contribution, $C_{w,0}$ and $C_{w,Pb}$ are the weighted counts resulting from measurements without sample and with a ^{208}Pb sample, respectively. They have been derived with the weighting function of the uranium sample. The last term in Eq. 4 accounts for the contribution of neutron sensitivity of the C_6D_6 detection system. The correction factor R_n is the ratio of the neutron scattering yield of the ^{238}U and ^{208}Pb sample. The factors $k_1 = 1.00 \pm 0.03$ and $k_2 = 1.00 \pm 0.05$ are used to introduce uncertainties due to systematic effects in the background model. These values together with their uncertainties were obtained from a comparison of the background based on Eq. (4) and the background dips present in the TOF spectra due to the fixed black resonance filters and in the spectra resulting from additional measurements with Ag, W and Co black resonance filters. The weighted response together with the total background estimated by Eq. 4 is shown in Fig. 2. This figure shows that in the URR, at energies above 10 keV, the uncertainty on the capture yield is dominated by the uncertainty on the background.

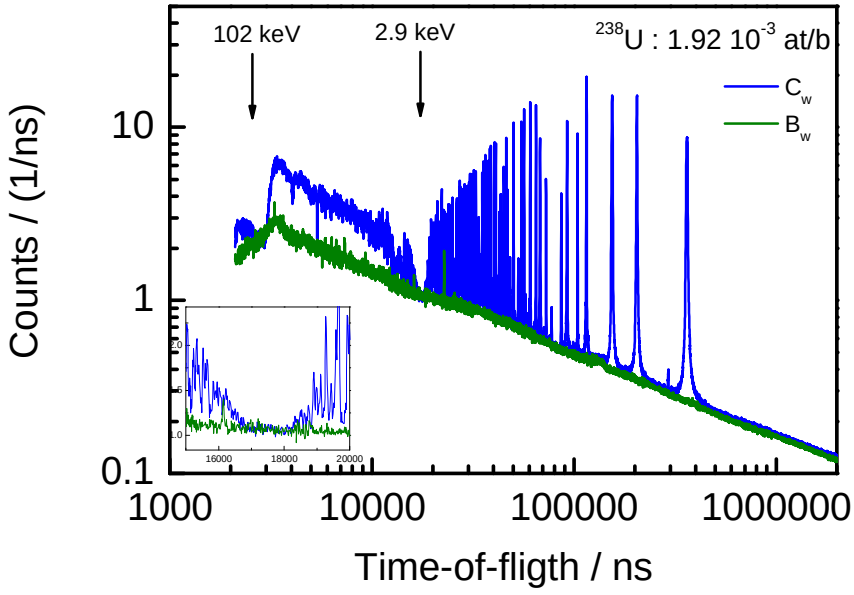

Fig.2 Weighted response of the C_6D_6 detection system at a 12.5 m station of GELINA for measurements with a ^{238}U sample (areal density = 1.92 10^{-3} at/b) and the background contributions estimated by Eq. 4. The dip at the

black resonance at 2.9 keV is due to the presence of a fixed Na filter, which is used to reduce bias effects due to the background correction.

The background for the flux measurements is derived from an analytical expression applying the black resonance technique [7]. The analytical function was a sum of a time independent and two time dependent components:

$$B_\varphi(t_m) = k_\varphi(a_0 + a_1 t_m^{\lambda_1} + a_2(t_m + t_0)^{\lambda_2}) \quad , \qquad (5)$$

The time dependence of the background was derived from saturated resonance dips created by black resonances of Ag, W, Co, Na, and S filters. The last term accounts for the contribution of overlap neutrons. This contribution was estimated by an extrapolation of the TOF spectrum at the end of the cycle. It is approximated by a power function, where the fixed time offset t_0 is equal to the spacing between the electron bursts. For an operating frequency of 800 Hz, the parameter t_0 is 1.25 ms. For each configuration the amplitudes a_1 and a_2 were adjusted to the black resonance dips at 2.85 keV and 102 keV due to the fixed Na and S filters to account for the impact of the presence of the samples and background filters [7]. The factor k_φ is introduced to account for an uncertainty of the model with k_φ=1.00 ± 0.03.

The zero point of the time scale was deduced from the position of the γ-ray flash with an uncertainty of 1 ns. The flight path length of the transmission station was calibrated using low energy resonances of ^{238}U + n determined by Derrien et al. [25].

The well-isolated and saturated peak of the 6.673 eV resonance was used to determine the normalization factor N_c in Eq. 2 by a fit to the experimental data. The result of a least squares adjustment to determine the normalization factor is shown in Fig. 3. For this resonance the neutron width is much smaller compared to the radiation width. Therefore, when the fit is restricted to the saturated resonance profile, the normalization factor can be derived independent of the resonance parameters as demonstrated in Ref. [7, 28]. In addition, when an internal normalization is applied, i.e. using a resonance of the nucleus under investigation, the experimental conditions remain unchanged and bias systematic effects are largely reduced [7]. It has been demonstrated in Ref. [28] that under these conditions the normalization factor N_c can be derived with an uncertainty of less than 1.7%, when the ^{10}B(n,α) is used as neutron cross section standard for the flux measurement and in the application of the weighting function both the neutron and γ-ray transport in the sample is taken into account as described in Ref. [7, 8]. Part of this uncertainty is due to the fact that the prompt γ-ray emission spectrum of the normalization resonance is different from the spectrum in the energy region of interest. Hence, the uncertainty can still be reduced to less than 1% when the spectrum of the normalization resonance is similar to the one of the reaction being studied, as discussed in Ref. [7].

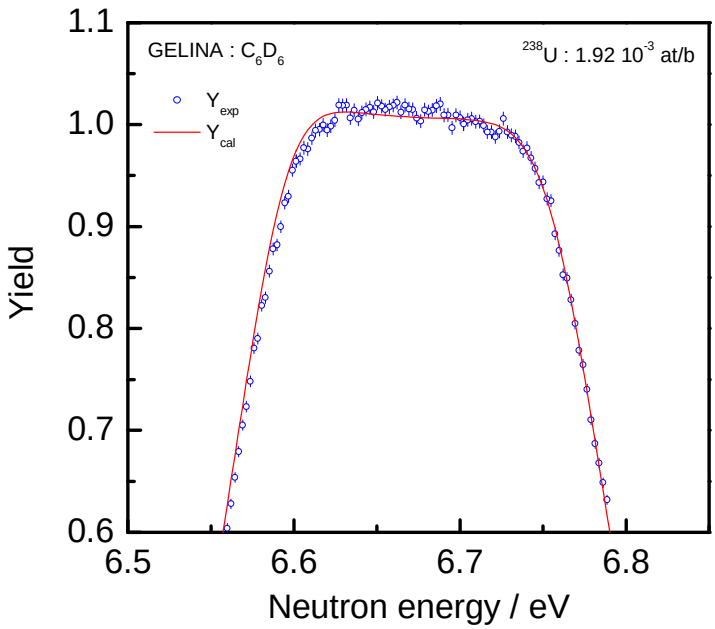

Fig. 3 Experimental capture yield around the 6.67 eV resonance obtained with the C_6D_6 detection system installed at a 12.5 m station of GELINA together with a the result of least squares adjustment to determine the normalization factor.

3.3 Results

By performing the data reduction with AGS the experimental transmission T_{exp} and capture yield Y_{exp} were derived together with a propagation of all uncertainty components. The uncorrelated uncertainties due to counting statistics in the TOF-spectra and the correlated components introduced by the uncertainties on the factors (N_T, k_T) and (N_c, k_1, k_2, k_φ) on T_{exp} and Y_{exp}, respectively, are propagated and separately reported. The experimental transmission and capture yield can be used in a least squares adjustment to derive the resonance parameters. To avoid bias effects due to a problem known as Peelle's Pertinent Puzzle (PPP), see e.g. d'Agostini [30], only uncorrelated uncertainties should be included in the fit to the data [7]. Bias effects due to PPP can be introduced when resonance structured data in the URR are fitted and correlated uncertainties are included in the least squares adjustment as demonstrated in Ref. [7]. To propagate all uncertainty components and determine the full covariance matrix of the parameters, different methods, i.e. conventional uncertainty propagation, Monte Carlo sampling or marginalization, can be applied as discussed in Ref.[7, 31]. As shown in Ref. [7] the most conservative uncertainties are obtained from Monte Carlo sampling.

At GELINA the REFIT code [32] is used to derive the parameters of individual resonances in a fit to the data, in other terms by a resonance shape analysis (RSA) of the experimental data. The code is based on the Reich-Moore approximation of the R-matrix nuclear reaction theory [33]. It accounts for various experimental effects such Doppler broadening, the response function of the TOF-spectrometer, neutron self-shielding, multiple interactions in the sample, the impact of γ-ray transport in the sample and the neutron sensitivity of the capture detection system [34]. The latest version also includes models to account for sample inhomogeneities [35].

The experimental yield below 100 keV is obtained with a normalization uncertainty of 1%. This uncertainty includes the uncertainty on the shape of the neutron flux, which can practically be neglected as explained in Ref. [7]. Due to the limited resolution at the 12.5m station a RSA of the data is limited to about 800 eV. In Fig. 4 the experimental yield is compared with the one calculated by REFIT using the resonance parameters derived by Derrien et al. [25]. At energies below 150 eV there is a good agreement between experimental and calculated yield is good. However, at higher energies adjustments to the parameters are required to describe the data on a 1- 2% level. The yield in the URR can be used to derive an average capture cross section between 5 keV and 100 keV. Based on the values for k_1 and k_2, together with the signal to background ratio shown in Fig.2, a combined uncertainty of about 2.5% is estimated for the capture yield in the URR. This uncertainty is higher compared the one for ^{232}Th(n,γ) in Ref. [28]. This is due to the less favorable signal to background conditions mainly due to the difference in sample properties.

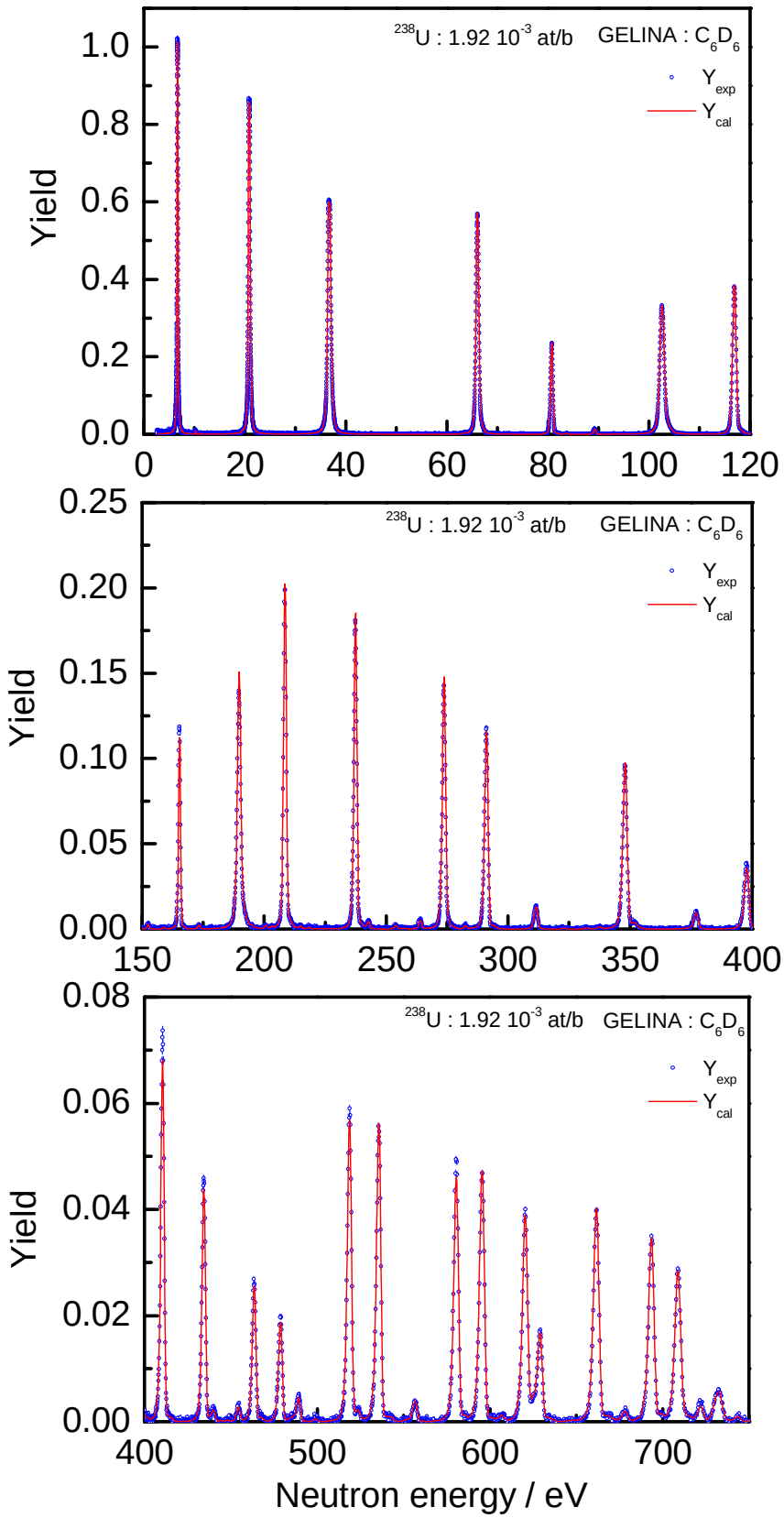

Fig.4 Experimental yield Y_{exp} of a ^{238}U sample with an areal density of 1.92 10^{-3} resulting from measurements at GELINA with a C_6D_6 detection system. The experimental data are compared with the corresponding theoretical yield Y_{cal} derived with REFIT using the parameters of Derrien et al. [25].

An additional confirmation of the parameters of Derrien et al. [25] in the low energy region is given in Fig.5, where the experimental yield around the 36.68 eV resonance is compared with two theoretical yields calculated with the MCNP5 code (version 1.40) using the ENDF/B-VII.1 data file. Given the thickness of the target and the ratio between the radiation and neutron width, the yield around the 36.68 eV resonance is sensitive to the treatment of the Doppler broadened Double Differential Cross Section (DDXS) as discussed in Ref. [36]. Becker et al. [37] developed a practical formalism, referred to as Doppler Broadened Rejection Correction (DBRC), which allows for a relatively simple implementation of the resonance and temperature effects on the calculated DDXS. To show the impact of the DDXS on the observed profile, the yield was calculated with a standard version of MCNP5 applying the asymptotic DDXS above 10 eV at 300 K and a modified version of MCNP5 which included the DBRC formalism. The results in Fig. 5 reveal that the resonant dependent DDXS model implemented in DBRC is needed to correctly describe the observed profile. In addition, since the profile is sensitive to both the scattering and capture reaction, the good agreement between the calculated and experimental yield in case of DBRC confirms the parameters for this resonance derived by Derrien et al. [25]. The small differences at the low TOF side (high energy) of the resonance are most probably due to additional experimental effects which are not included in the model [37].

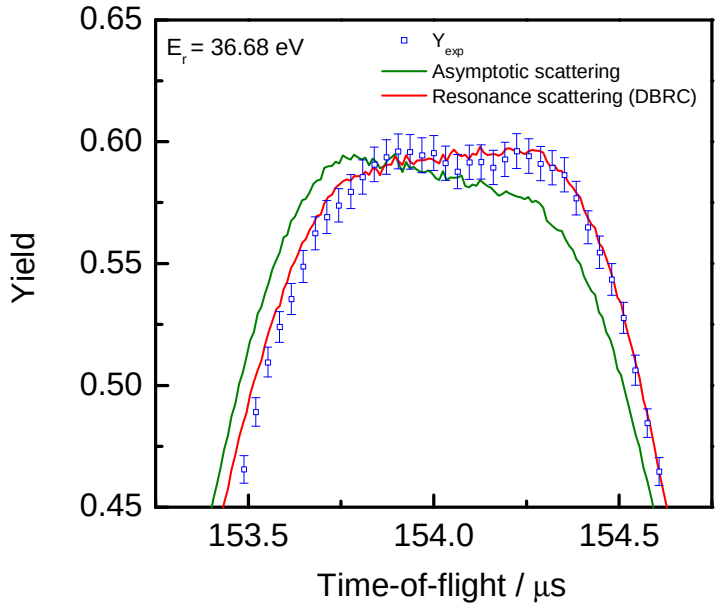

Fig.5 Experimental yield around the 36.68 eV resonance obtained at a 12.5 m station of GELINA using a ^{238}U sample with an areal density of 1.92 10^{-3} at/b The yield is compared with a theoretical yield calculated with MCNP5 applying the asymptotic DDXS (Double differential cross section) and with a modified version of MCNP5 which included the DBRC formalism described by Becker et al. [37].

4. Measurements at the n_TOF facility of CERN

At the n_TOF facility neutrons are generated in spallation reactions by a pulsed 20 GeV/c proton beam impinging on a lead block (see Fig. 6). The Pb target is surrounded by 5 cm of water and borated water, serving as a coolant and as a moderator of the originally fast neutron spectrum [38]. The resulting white neutron flux ranges from thermal energies to 1 GeV, with a nearly isolethargic flux dependence up to 100 keV. The neutrons travel through an evacuated beam line to the experimental area at a distance of 185 m from the spallation target, where the sample and the detectors are placed. The neutron flux at n_TOF is continuously monitored by a thin neutron ^{6}Li foil that is placed in the beam and viewed by a silicon detector [39]. The experimental program at n_TOF includes measurements of fission cross-sections performed with Parallel Plate Avalanche Counters (PPAC) and MicroMegas (MGAS) detectors, and of capture cross-sections studied either with total energy detectors C_6D_6 [9] or with a total γ-ray absorption detector (TAC) [10, 40, 41]. An overview of the n_TOF facility and the various measuring devices is given in Ref. [38].

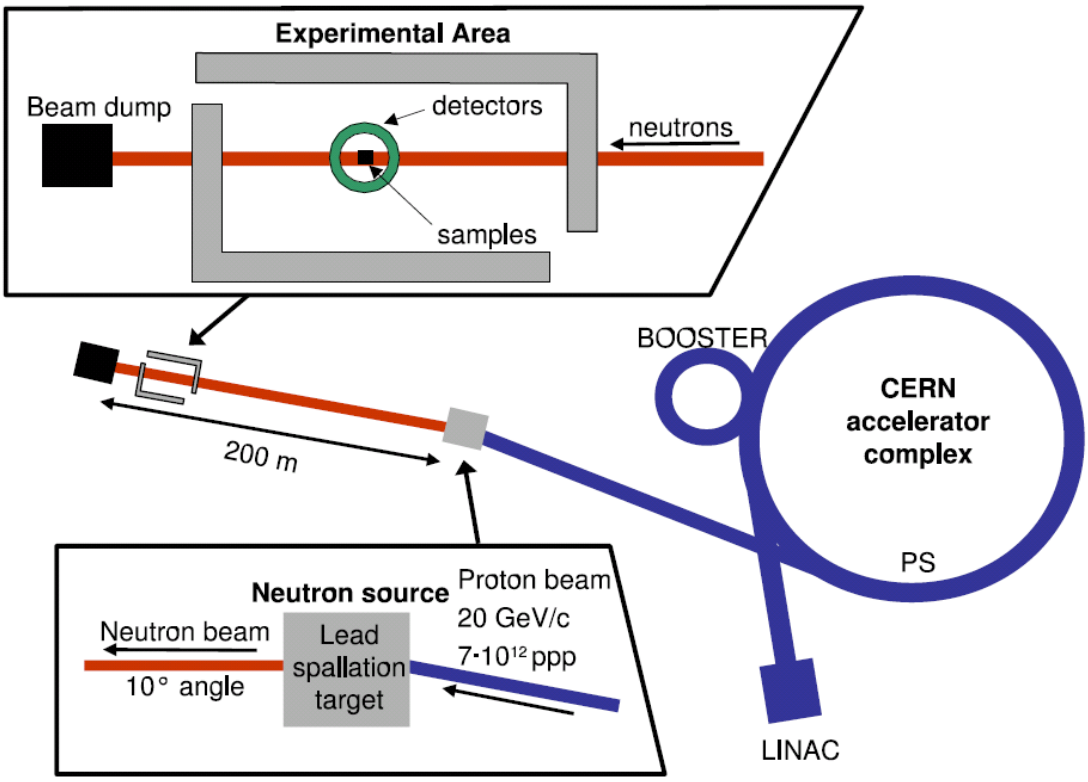

Fig. 6 Layout of the n_TOF facility within the CERN accelerator complex. A LINAC feeds the PS-booster, which provides the PS (Proton Synchrotron) with protons of 1.4 GeV/c for acceleration up to 20 GeV/c. This beam is extracted and sent to the n_TOF lead spallation target in bunches of 7 10^{12} protons. The experimental hall is located near the end of the 200 m long neutron beam line.

The data acquisition of the detection systems at n_TOF is based on a fully digitized system, which is described in detail in Ref. [42]. The signals of each detector are recorded with 8 bits resolution and 8MB memory. The sampling rate can vary between 100 MHz and 500 MHz, depending on the neutron energy region of interest. Correspondingly, the system can record from 80 ms to 16 ms long data buffers containing the digitized response of each detector. The digitized signals are already analyzed online and a list mode data file is produced containing the energy deposited (or light output for a scintillator) in the detector, a time tag and detector identification number. For events recorded in the BaF_2 detectors a particle identification (photon or α) is added and the data from the individual detectors is analyzed to derive the total number of events in a given coincidence window. This number (or crystal multiplicity) is also included in the list mode data file.

As discussed in section 2, results obtained with the C_6D_6 and TAC are complementary. The TAC has a high detection efficiency and powerful background rejection capabilities. However, these favorable conditions are only valid for neutron energies below 10 keV. Above 10 keV the detection system suffers from the influence of the γ-ray flash. In the energy region above a few keV, the use of low efficient C_6D_6 detectors with their low intrinsic neutron sensitivity is preferred. Therefore, capture cross section measurements with the two systems were carried out at n_TOF.

4.1 Sample properties

The ^{238}U sample with label (1) in Table 1, which was produced and characterized at the EC-JRC-IRMM, was used for the measurements with both the C_6D_6 and the TAC. In addition to the measurement with the ^{238}U sample, measurements without sample and with ^{nat}C, ^{nat}Ag, ^{nat}Fe and ^{nat}Pb samples were carried out to determine the background and verify the normalization of the data. To comply with the radiation protection regulations at CERN, the ^{238}U sample was encased in a 60-μm thick aluminum foil and a kapton foil of about 75 μm thickness, as illustrated in Fig. 7. The characteristics of the samples used during the measurement campaigns at n_TOF are given in Table 2, together with the total number of protons used for the measurements.

Fig. 7 Samples measured at n_TOF: ^{nat}C (top), ^{238}U(left) and ^{197}Au(bottom). The ^{238}U sample was encased in a 60-μm thick aluminum foil and a 75-μm thick kapton foil.

Table 2 Characteristics of the samples used in the capture measurements together with total number of protons produced during the measurements.

Sample	Size mm x mm	Mass g	Areal density at/b	Total number of protons		
				C_6D_6		TAC
				no filters	filters	no filters
^{238}U	53.67 x 30.21	6.125 ± 0.002	(9.557 ± 0.050) 10^{-4}	7.85 10^{17}	7.03 10^{17}	4.12 10^{17}
no sample						1.05 10^{17}
^{197}Au	53.30 x 30.00	1.547	2.07 10^{-4}			6.74 10^{16}
^{nat}C	53.35 x 30.65	14.638	4.49 10^{-2}			7.05 10^{16}
no sample				6.27 10^{16}	1.64 10^{17}	
Al+kapton				9.65 10^{16}	4.17 10^{17}	
^{197}Au	53.30 x 29.65	9.213	1.77 10^{-3}	1.32 10^{17}	9.93 10^{16}	
^{nat}C	53.55 x 30.20	28.89	8.94 10^{-2}	2.43 10^{17}	2.77 10^{17}	
^{nat}Fe	53.71 x 30.22	3.225	2.13 10^{-3}	9.85 10^{16}	1.17 10^{17}	
^{nat}Ag	53.75 x 30.30	4.620	1.59 10^{-3}	1.60 10^{16}		
^{nat}Pb	53.77 x 30.10	9.440	1.73 10^{-3}	1.50 10^{17}	1.53 10^{17}	

4.2 Capture experiments with C_6D_6 detectors

4.2.1 Experimental conditions

To apply the total energy detection principle at n_TOF, a detection system consisting of two C_6D_6 detectors was used (see Fig. 8). The detectors were placed opposite to each other at 90^o with respect to the direction of the neutron beam and 9 cm upstream from the sample. A commercial available BICRON detector and a custom made detector [43] were used. The detectors and the sample holder material were optimized to have a low sensitivity to γ-rays resulting from neutron capture in the detector and the surrounding materials.

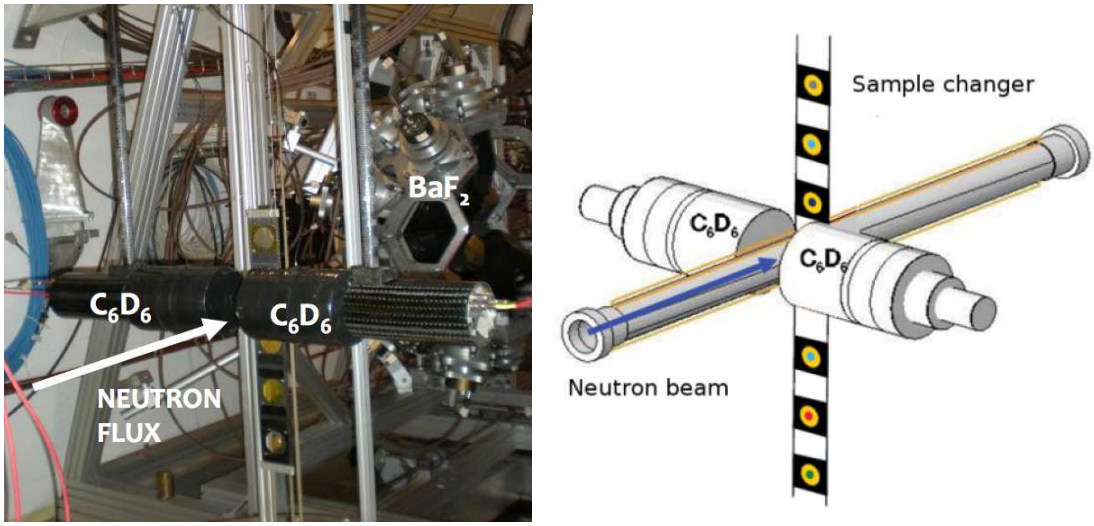

Fig. 8 C_6D_6 detection system installed at n_TOF. The experimental set-up as installed at n_TOF (left) is shown together with the details of the geometry input file (right) used for the simulations.

To calibrate the light output of the C_6D_6 scintillators into a signal expressed in an energy scale, measurements with γ-ray radionuclide sources (^{137}Cs, ^{88}Y and an AmBe source) were used. The stability of the neutron beam, silicon beam monitor and C_6D_6 detectors was verified and only runs with stable conditions of the detectors and neutron beam were selected as discussed in Ref. [5].

Apart from measurements with the uranium sample, the experiment included additional runs using an empty sample cavity, only the sample holder and a carbon and a ^{nat}Pb sample. Some of the measurements were also repeated with black resonance filters (W, Co and Al) in the beam. All these measurements were carried out to determine the background correction for the C_6D_6 system.

4.2.2 Data reduction

The list mode data were sorted into TOF-histograms after application of the weighting function. Each event recorded in the C_6D_6 detectors was weighted using a weighting function which was determined by Monte Carlo simulations as described in Ref. [9]. In the calculation of the weighting function the effect of the discrimination level was taken into account and the γ-rays were supposed to be homogeneously distributed in the sample. For the analysis of the first three strong resonances a second weighting function was applied. This weighting function was derived for a γ-ray distribution which follows the exponential attenuation of the neutron beam in the sample.

The experimental yield Y_{exp} was derived from the response of the capture detection system and the neutron flux:

$$Y_{exp} = \frac{1}{f_b\,\varepsilon_c}\frac{C_w - B_w}{\varphi}, \qquad (6)$$

where C_w is the dead time corrected weighted TOF-spectrum per proton pulse obtained with the ^{238}U sample and B_w the corresponding background contribution. The incoming neutron flux per proton pulse is denoted by φ, ε_c is the detection efficiency to detect a capture event and f_b is the fraction of the neutron beam intercepted by the sample. The neutron flux was derived from the response in the silicon neutron monitors.

The response of the C_6D_6 system at n_TOF suffers from similar background contributions as the C_6D_6 system at GELINA, as discussed in section 3.2.2 and Ref. [7]. However, due to the difference in type of neutron source an additional component resulting from in-beam γ-rays has to be taken into account. To evaluate the background a series of measurements under different conditions have been carried out. Fig. 9 shows the TOF-spectra obtained with the ^{238}U sample together with the total background. At high TOF (low energies) the contribution of the time-independent component is dominating. At low TOF (high energies) the background is mainly due to in-beam γ-rays. This component was derived from measurements with a Pb sample. Due to the low neutron sensitivity of the detection system the contribution due to neutron scattering in the sample can be neglected. This contribution was estimated as in Eq. 4 using the response to a carbon sample.

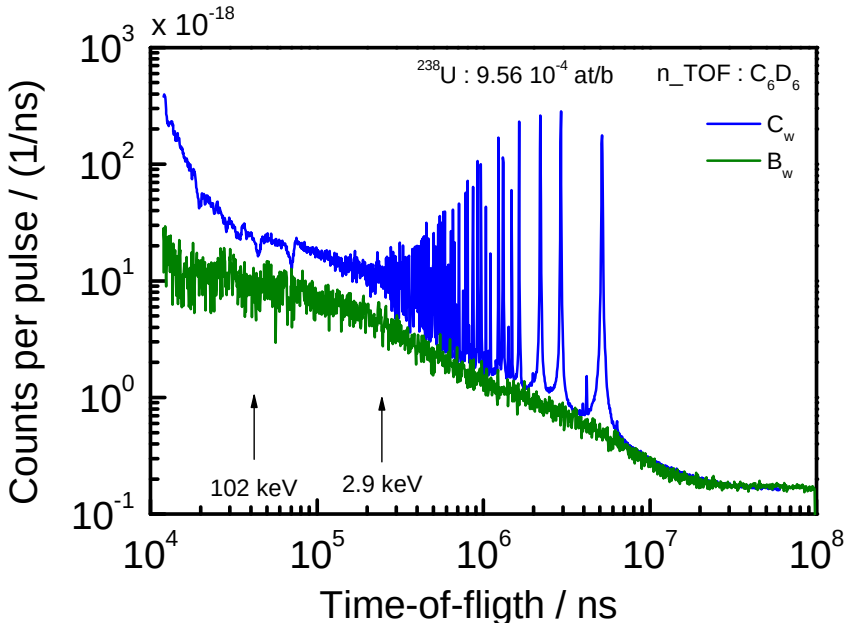

Fig. 9 Weighted response for measurement with a ^{238}U sample (areal density = 9. 10^{-4} at/b) (C_w) using the C_6D_6 system installed at n_TOF. The background contribution (B_w), which was estimated by Eq. 4 with an additional term to account for the contribution of the in-beam γ-rays, is also shown.

The zero point of the time scale was deduced from the position of the γ-ray flash. The flight path length was calibrated using low energy s-wave resonances of of ^{238}U + n determined by Derrien et al. [25].

Since it is difficult to determine accurately the beam interception factor and the detection efficiency, they were lumped into one normalization factor $N_c = 1 / (f_b\, \varepsilon_c)$. The normalization factor N_c was derived from a resonance shape analysis of the saturated resonance at 6.673 eV using SAMMY [44]. An example of such an analysis is shown in Fig. 10. As discussed in section 3.2.2 and Ref. [7], such a procedure reduces the uncertainty on the normalization to less than 1%. In addition, a measurement of the absolute neutron flux is not required [7]. However, to link this normalization to other energy regions, the beam interception factor is supposed to be energy independent and an accurate energy dependence of the neutron flux is required. Therefore, the uncertainty on the experimental yield is mainly due to the uncertainty on the energy dependence of the neutron flux which is 1% below 1 keV and 2% between 1 keV and 10 keV.

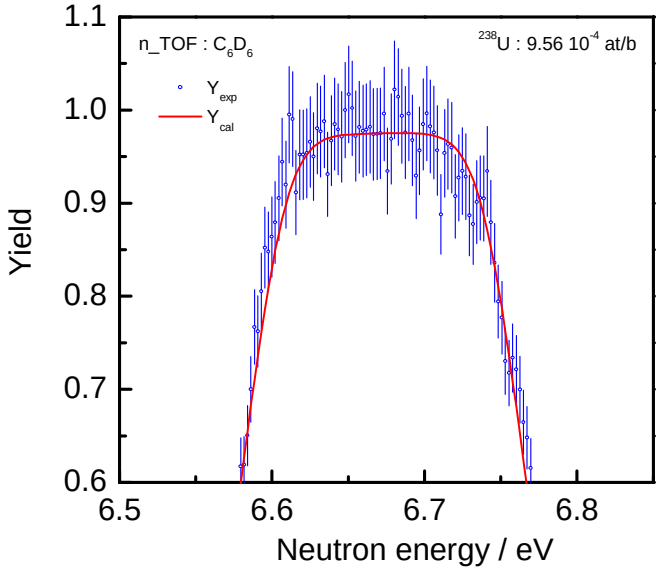

Fig. 10 Experimental capture yield around the 6.67 eV resonance resulting from measurements with the C_6D_6 detection system installed at n_TOF together with the result of a least squares adjustment with SAMMY to determine the normalization factor.

4.3 Capture experiments with the BaF_2 total absorption detector

4.3.1 Experimental conditions

The total γ-ray absorption detector installed at n_TOF [10, 40, 41] is a segmented 4π detector array made of 40 BaF_2 crystals, as shown in Fig. 11. Due to the large solid angle coverage and high efficiency for detecting γ-rays, the efficiency to detect a capture event is almost 100%. To reduce the background induced from neutrons scattered in the sample, each crystal is surrounded by a ^{10}B loaded carbon fibre capsule and the sample by a borated polyethylene neutron absorber. The neutron absorber material was selected to minimize the background due to scattered neutrons using the Geant4 Monte Carlo code. A detailed description of the TAC can be found in Ref. [41].

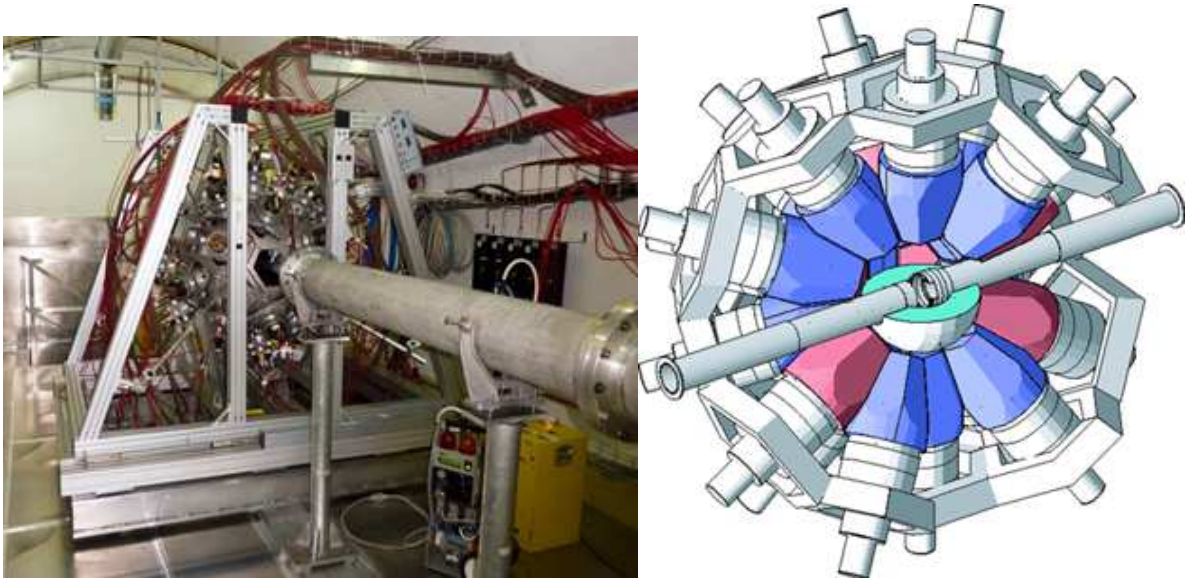

Fig. 11 BaF_2 based total absorption detection system installed at n_TOF. The experimental set-up (left) is shown together with the details of the geometry input file (right) used for the simulations with Geant4.

For all 40 BaF_2 crystals the light output was calibrated in terms of electron equivalent energy and the resolution as a function of light output was determined by measurements with three radionuclide γ-ray sources (^{137}Cs, ^{88}Y and AmBe). In addition the time outputs for the BaF_2 crystals linked to a flash-ADC digitizer were aligned within 2 ppm based on time coincidence measurements with a ^{88}Y γ-ray source. After this alignment a coincidence window of 20 ns was applied.

Due to the large amount of ^{238}U, dead time and pile-up effects influence the results. To study these effects experiments at three different beam intensities were carried out and correction procedures verified. Applying the procedures described in Ref. [45, 46], bias effects due to pile-up and dead time were reduced to less than 1%. This is illustrated in in Fig. 12, where the counts normalized to the total number of incident proton pulses are given resulting from measurements with two incident beam intensities (low ≈ 0.6 10^{12} protons per pulse and medium ≈ 1.1 10^{12} protons per pulse). The normalized counts before and after dead time correction are shown around the peaks of the 6.67 eV, 20.86 eV and 66.02 eV resonances. Without any correction the counts in the peak for medium intensity differ from those for low intensity by 3.4%, 6.25% and 8.3% for the 6.67 eV, 20.86 eV and 66.02 eV resonances, respectively. This systematic difference is reduced to less than 1% after applying the correction procedures of Ref. [45, 46]. The low energy wing of the 66.02 eV resonance reveals that after application of the corrections also a better agreement between the shape of the resonance is obtained.

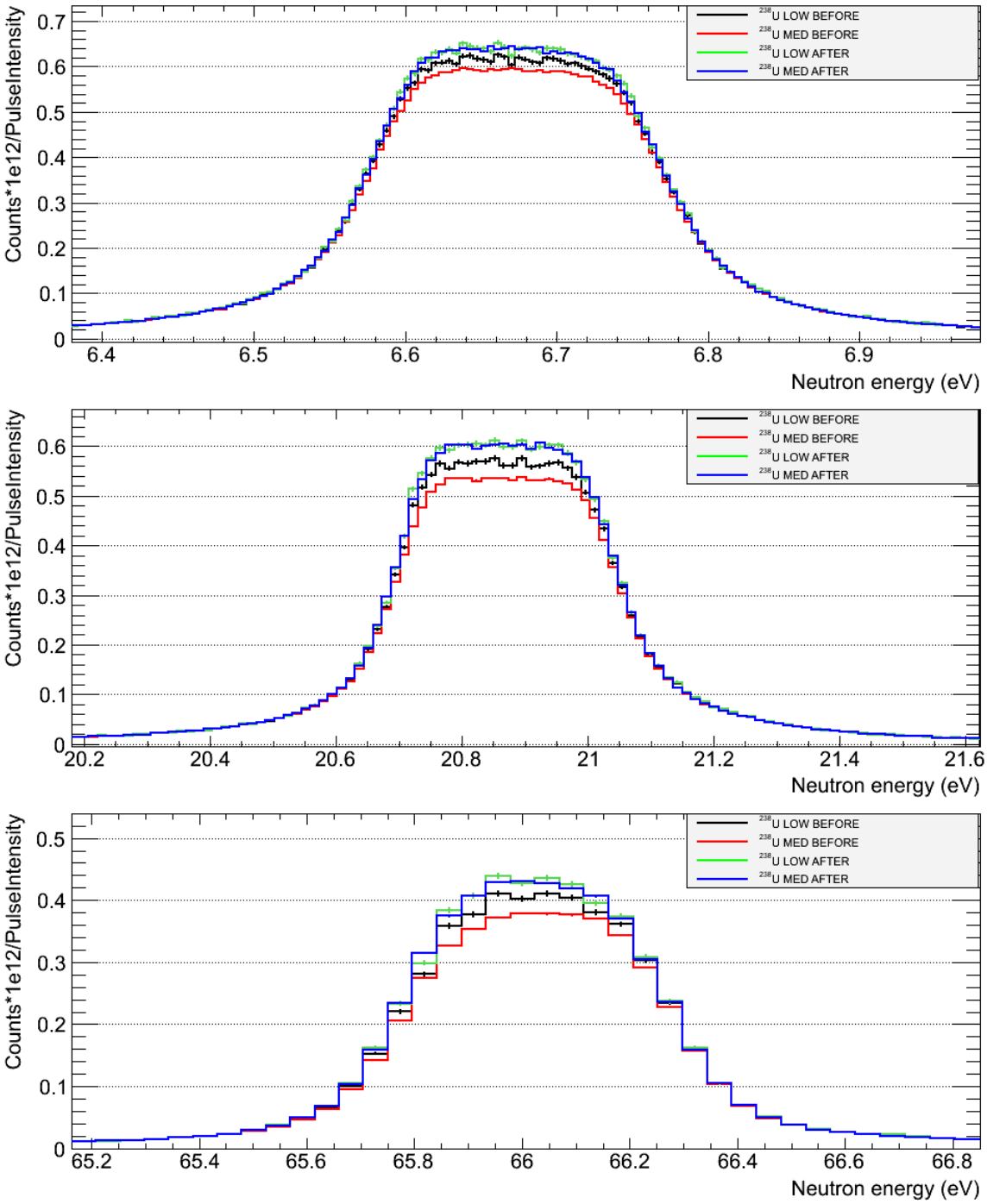

Fig. 12 Illustration of the effect of the correction for dead time. The response with and without application of the correction is shown for the peaks of the resonances at 6.67 eV, 20.86 eV and 66.02 eV. The results are shown for a low and medium beam intensity. Details on the correction procedures can be found in Ref. [45, 46].

To study the different background components, measurements with a carbon sample and without sample were performed. The time independent component was verified by measurements without beam, with and without the ^{238}U sample in place. The analysis procedures were verified by measurements with a ^{197}Au sample. The total measurement campaign lasted 41 days.

4.3.2 Data reduction

The list mode data were sorted into TOF-histograms after the 40 detectors were calibrated for their time and light output. The experimental yield Y_{exp} was derived based on Eq.6 using the response of the capture detection system, which was corrected for dead time and background, and the neutron flux of Ref. [38]. The neutron flux in Ref. [38] has been characterized using different detection systems and based on standard cross sections for neutron induced reactions.

The BaF_2 suffers from similar background contributions as discussed in section 3.2.2 and in Ref. [7]. One of the advantages of a total absorption detector is that the signal to background can be optimized by putting a constraint on the multiplicity and total energy (or light output) of the events [10, 40]. For the ^{238}U measurements the best compromise between minimizing the background and maximizing the efficiency was found for multiplicities ≥ 2 and a total light output between 2.5 MeV and 5.75 MeV. The lower energy limit is set to eliminate the contribution of the 478 keV and 2.2 MeV γ-ray resulting from the $^{10}B(n,\alpha\gamma)$ and $^{1}H(n,\gamma)$ reaction. Due to this selection the time dependent component due to γ-rays scattered by the sample is largely reduced. The time independent background contribution was estimated by measurements without beam, with and without the ^{238}U sample present in the detector. The sample independent time dependent component was derived from measurements with the beam and no sample. The background due to scattered neutrons was estimated by two procedures. A procedure similar to the one described in section 3.3.2 using a carbon sample and a procedure based on the difference in the full energy that is deposited by a γ-ray resulting from a $^{238}U(n,\gamma)$ event and a γ-ray resulting from capture in the BaF_2 detector [7, 10, 40]. It was shown that the first method applied for the BaF_2 might overestimate the background by a factor of two. This is due to the fact that in the first method it is difficult to separate the direct from the delayed contribution discussed in section 3.2.2. The latter cannot be neglected for a total absorption detector. However, it is difficult to determine and has partly lost the correlation in time. Therefore, the second method was applied to calculate the final yield. The final response together with the background components is shown in Fig. 13.

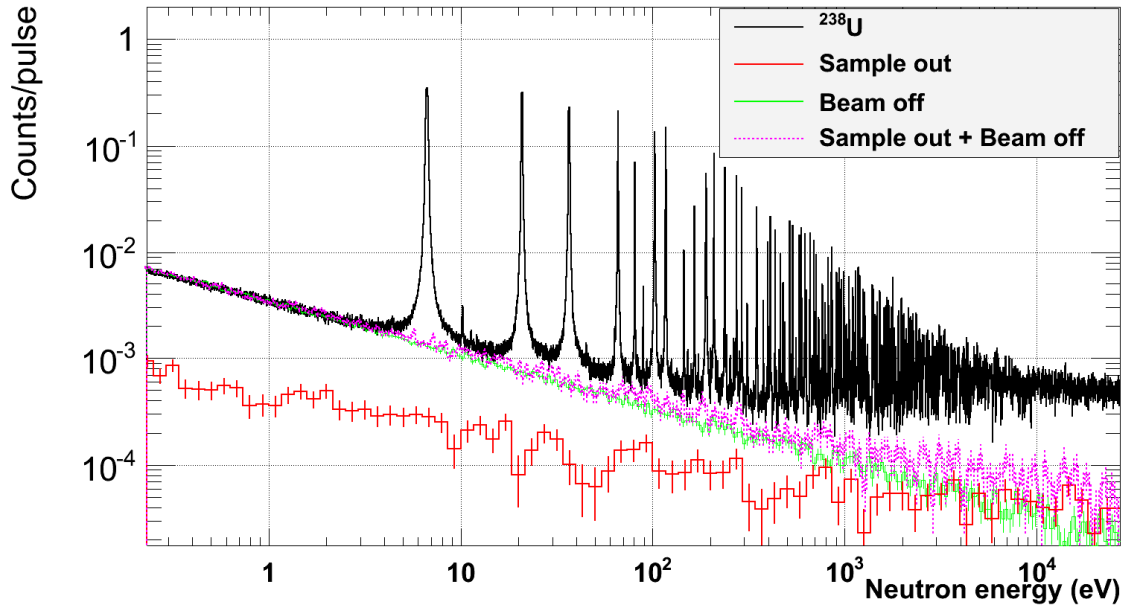

Fig. 13 Response of the TAC for measurements at n_TOF with a ^{238}U sample (areal density = 9.56 10^{-4} at/b) and the background contributions due to the time independent (green) and time dependent background (red) components. The sum of these components is also given (purple).

The zero point of the time scale and the flight path length were derived from ^{238}U resonances below 1.2 keV. The energies of these resonances were taken from the JEFF 3.1.2 data library, which adopted the resonance parameters of Derrien et al. [25].

Similarly as for the C_6D_6, the data were normalized by lumping the beam interception factor and detection efficiency into one normalization factor N_c,, which was derived from a resonance shape analysis of the saturated resonance at 6.673 eV using SAMMY. An example of such an analysis is shown in Fig. 14. As discussed in section 3.2.2 and Ref. [7] such a procedure reduces the uncertainty on the normalization to less than 1%. Like the C_6D_6 data, the uncertainty on the experimental yield is mainly due to the uncertainty on the shape of the neutron flux which is 1% below 1 keV and 2% between 1 keV and 10 keV.

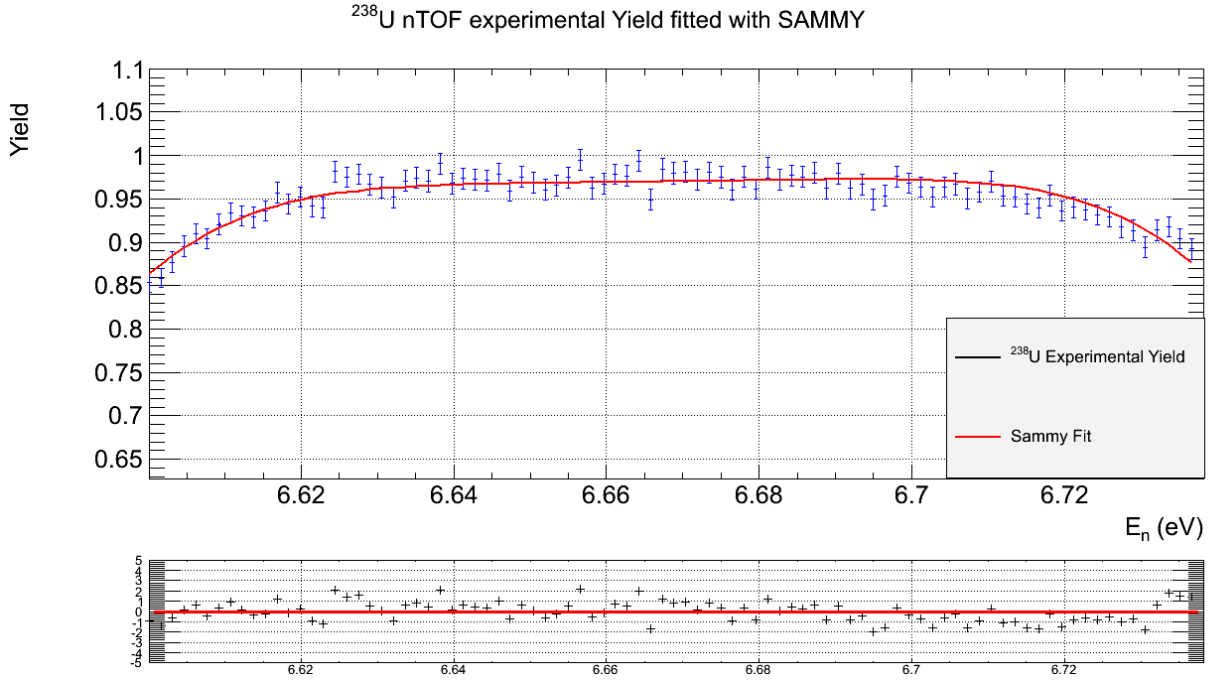

Fig. 14 Experimental capture yield around the 6.673 eV resonance resulting from measurements at n_TOF with the BaF_2 total absorption detector. The full line is the result of a least squares adjustment with SAMMY to determine the normalization factor.

4.4 Results

Capture yields for ^{238}U in the resonance region have been obtained from the measurements with the C_6D_6 detectors and TAC at n_TOF. Applying an internal normalization at the 6.673 eV saturated resonance the normalization uncertainty was reduced to less than 1%. This correlated uncertainty component has to be combined with an uncertainty of 1% below 1 keV and 2% between 1 keV and 10 keV due to the energy dependence of neutron flux. The yield derived from the measurements with the C_6D_6 are shown in Fig. 15 and Fig. 16. Those resulting from measurements with the TAC are given in Fig. 17. The experimental yields are compared with the theoretical yields calculated with SAMMY using the parameters of Derrien et al.[25]. The data from both the C_6D_6 detectors and TAC seem to confirm the conclusions made in section 3.3.

The results obtained with the C_6D_6 detector for energies below 750 eV seem compatible with those obtained at GELINA with a similar detection system. They confirm the observations made in section 3.3 that only for resonances above 200 eV a significant adjustment of the parameters are required. Above 250 eV the better resolution of the C_6D_6 data from n_TOF can be noticed. Therefore, the C_6D_6 data from n_TOF will contribute to an improved RSA up to about 3 keV. Above 3 keV the analysis will be hampered by limited counting statistics. However, as shown in Fig. 16 the data resulting from the TAC will complement the C_6D_6 data both above and below 3 keV. To derive an average capture cross section above 10 keV only the C_6D_6 data can be used. However, to arrive at a 2% level a more detailed study of the different background contributions is required.

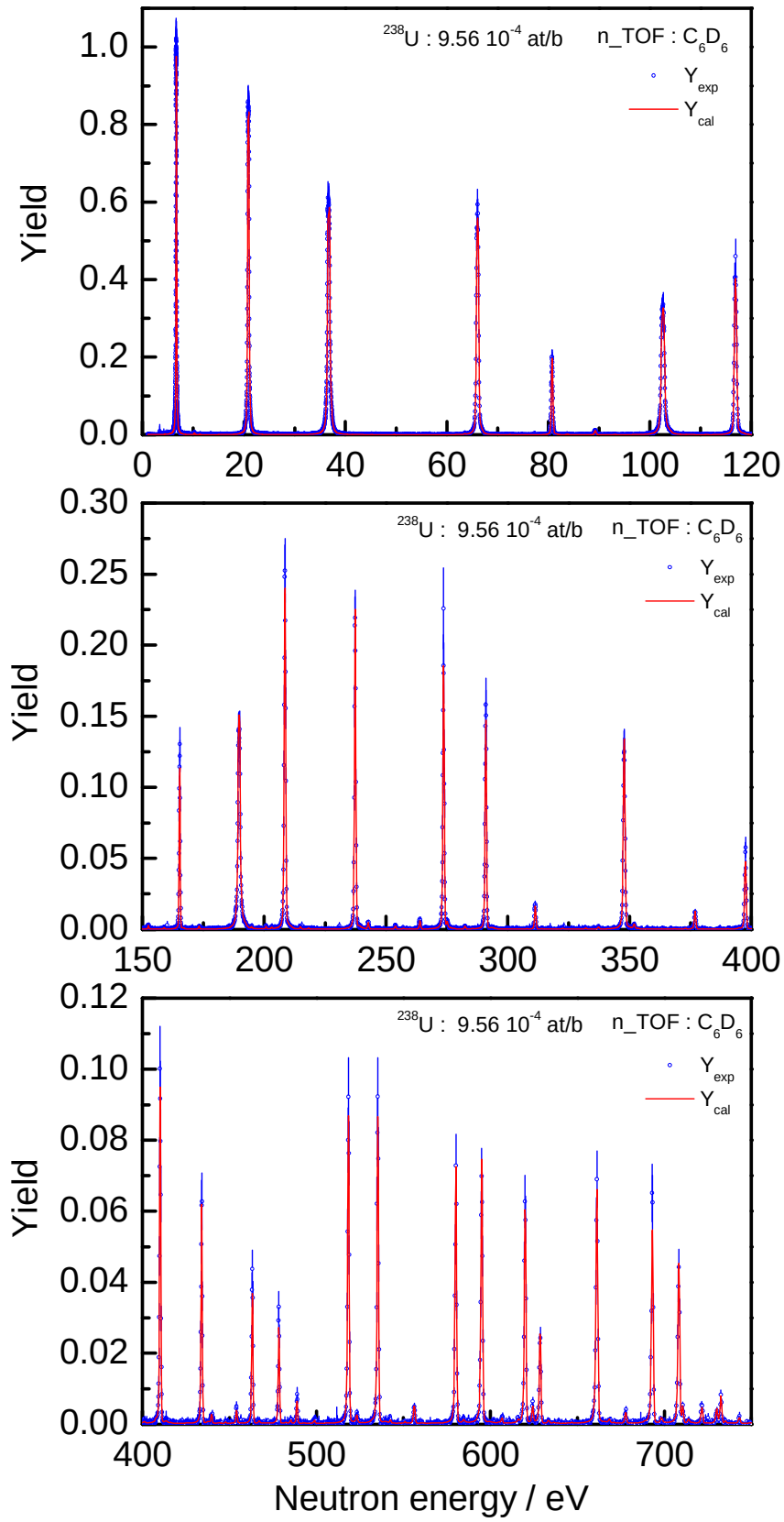

Fig. 15 Experimental yield Y_{exp} of a ^{238}U sample with an areal density of 9.56 10^{-4} at/b resulting from measurements at n_TOF with the C_6D_6 detectors. Experimental data below 750 eV are compared with the corresponding theoretical yield Y_{cal} derived with SAMMY using the parameters of Derrien et al. [25].

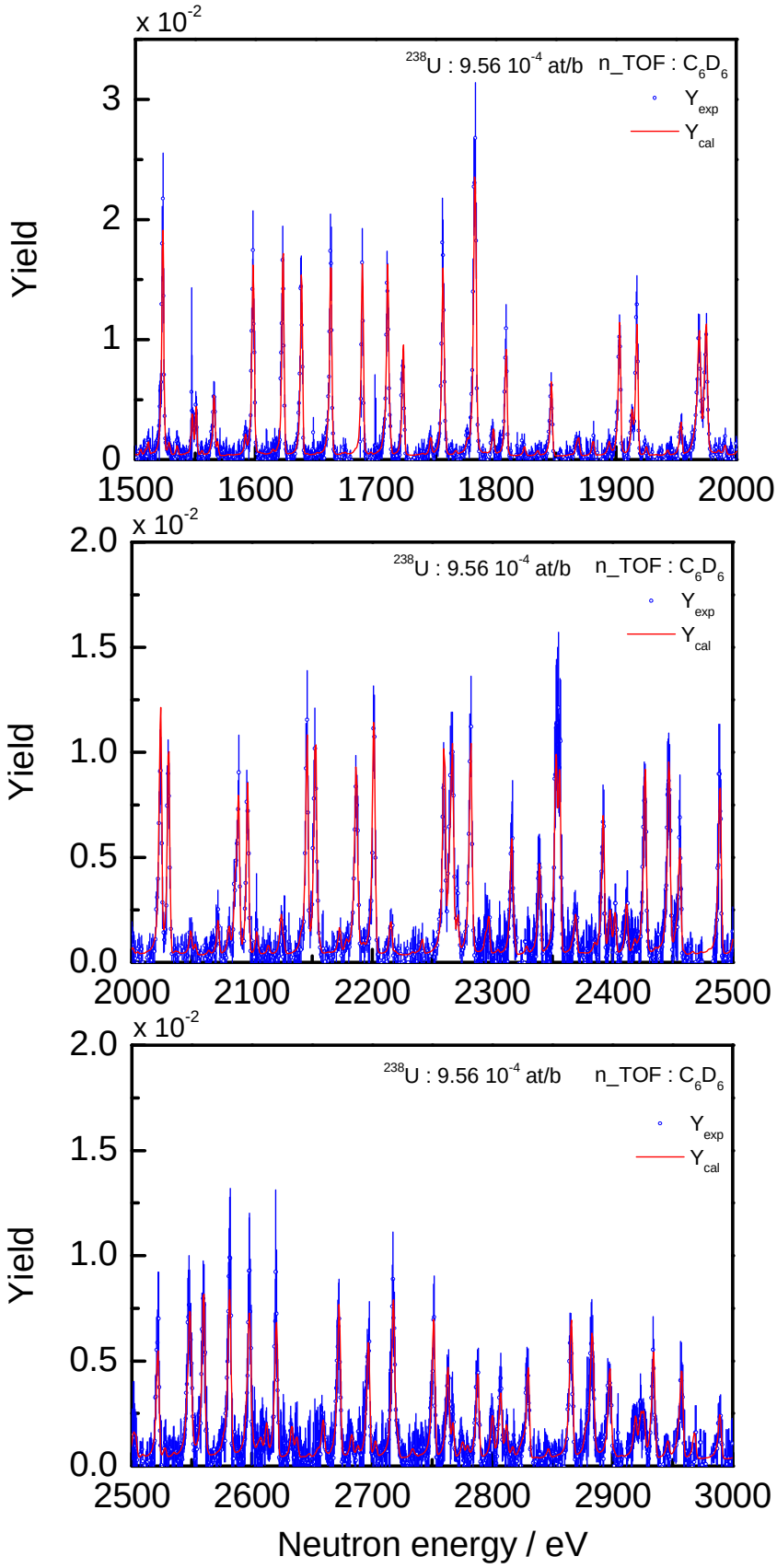

Fig. 16 Experimental yield Y_{exp} of a ^{238}U sample with an areal density of 9.56 10^{-4} at/b resulting from measurements at n_TOF with the C_6D_6 detectors. Experimental data between 1500 eV and 3000 eV are compared with the corresponding theoretical yield Y_{cal} derived with SAMMY using the parameters of Derrien et al. [25].

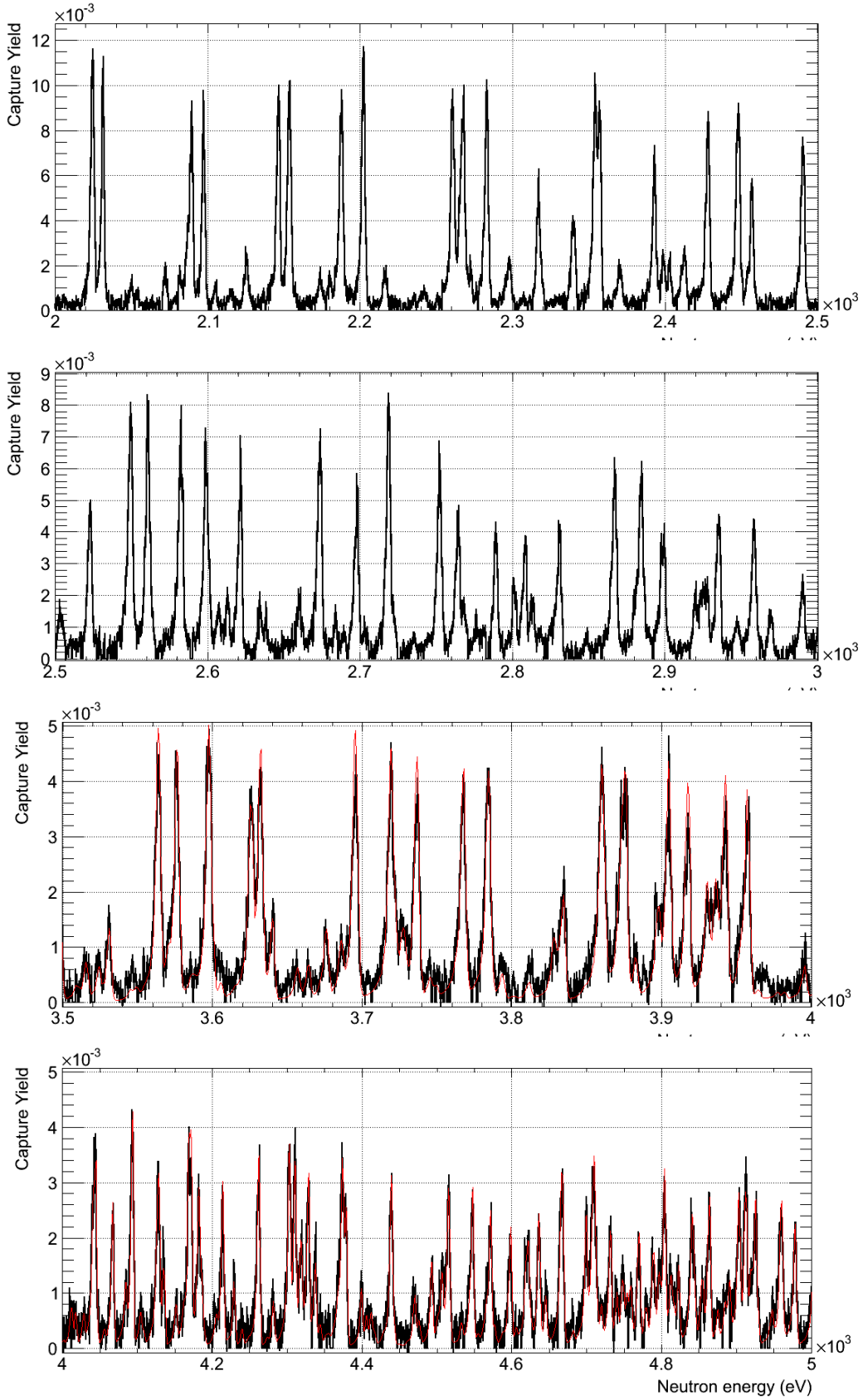

Fig. 17 Experimental yield Y_{exp} of a ^{238}U sample with an areal density of 9.56 10^{-4} at/b resulting from measurements at n_TOF with the BaF_2 total absorption detector. Experimental data between 3500 eV and 5000 eV are compared with the corresponding theoretical yield Y_{cal} derived with SAMMY using the parameters of Derrien et al. [25].

5. Summary and perspectives

To improve the capture cross section of ^{238}U in the resonance region, transmission and capture cross section measurements have been carried out at the time-of-flight (TOF) facilities GELINA and n_TOF. Complementary techniques have been applied to arrive at the targeted uncertainty between 1% and 2% for the capture cross section below 20 keV. Capture measurements with C_6D_6 detectors were carried out at GELINA and the resulting capture yield is given together with all uncertainty components following the AGS concept that is recommended by the Nuclear Data Section of the IAEA. The capture measurements were complemented with transmission measurements at a 50 m station of GELINA to verify the results of transmission data reported in the literature. At the n_TOF facility capture cross section measurements have been performed by applying the total energy principle with C_6D_6 detectors and the total absorption principle using an almost 4π detector consisting of 40 BaF_2 crystals. By a combined analysis of data resulting from measurements with complementary techniques at TOF-facilities with different resolution and background conditions it is possible to reduce the impact of bias effects on the final results.

At GELINA experimental capture yields were derived with a normalization uncertainty of 1% for neutron energies between 5 eV and 100 keV. The yields derived from measurements at n_TOF have a similar normalization uncertainty of 1%. This uncertainty has to be combined with an uncertainty of 1% below 1 keV and 2% between 1 keV and 10 keV due to the energy dependence of neutron flux. Above 200 eV the resolution at n_TOF is about a factor 4 better compared to the resolution at the 12.5 m station of GELINA. This improved resolution will be important for a resonance shape analysis of the data above 1 keV and will contribute to a reduction of the uncertainty of the resonance parameters. A comparison of the experimental yields obtained at both GELINA and n_TOF and calculated yields reveals that a re-evaluation of the resonance parameters is required to arrive at the target uncertainty specified in the High Priority Request List of the NEA/OECD. The experimental data obtained within the ANDES project together with transmission data reported in the literature can be used to re-evaluate the parameters of resonances below 10 keV. Given the uncertainties on the data such a re-evaluation will result in a capture cross section below 10 keV with an average uncertainty between 1% and 2%. For energies above 10 keV the average capture cross section will be mainly determined by the capture data obtained at GELINA and the results of the measurements with the C_6D_6 detectors at n_TOF. An uncertainty of 2.5% can be reached. This limit is mainly due to the impact of the background on the response of the C_6D_6 detector.

The results presented in this report demonstrate the successful completion of subtask 1.2.a and 1.2.c of the ANDES project. The outcome of these subtasks, i.e. deliverable D1.8, provides important experimental data to improve the capture cross section of ^{238}U. The data will be submitted to the EXFOR data base and will be used as an input for the CIELO project (Collaborative International Evaluated Library Organization), which has the capture cross section of ^{238}U in the resonance region as one of its priorities.

6. Dissemination activities

In this section dissemination of the activities of subtasks 1.2.a and 1.2.c of WP1 in the form of published papers and conference contributions are listed:

T. Wright, C. Guerrero, J. Billowes, T. Ware, D. Cano-Ott, E. Mendoza and the n_TOF collaboration, "High-precision measurement of the $^{238}U(n,\gamma)$ cross section at n_TOF, CERN", presented at the European Nuclear Conference, 9 – 12 December 2012, proceedings at
http://www.euronuclear.org/events/enc/enc2012/transactions.htm

R. Dagan, B. Becker, Y. Danon, F. Gunsing, S. Kopecky, C. Lampoudis, O. Litaize, M. Moxon and P. Schillebeeckx, "Impact of Doppler Broadened Double Differential Cross Section on Observed Resonance Profiles", presented at the International Conference on Nuclear Data for Science & Technology, New York, 4 – 8 March 2013, accepted for publication in Nuclear Data Sheets, January 2014.

C. Lampoudis, S. Kopecky, B. Becker, F. Gunsing, P. Schillebeeckx and R. Wynants, "^{238}U neutron capture cross section measurements in the unresolved resonance region at the GELINA facility", presented at the International Conference on Nuclear Data for Science & Technology, New York, 4 – 8 March 2013, accepted for publication in Nuclear Data Sheets, January 2014.

F. Mingrone, C. Massimi, G. Vannini and the n_TOF collaboration, "Measurement of the ^{238}U radiative capture cross section with C_6D_6 at the CERN n_TOF facility",, presented at the International Conference on Nuclear Data for Science & Technology, New York, 4 – 8 March 2013, accepted for publication in Nuclear Data Sheets, January 2014.

T. Wright, C. Guerrero, J. Billowes, T. Ware, D. Cano-Ott, E. Mendoza and the n_TOF collaboration, "High-precision measurement of the ^{238}U(n,γ) cross section with the Total Absorption Calorimeter (TAC) at n_TOF, CERN", presented at the International Conference on Nuclear Data for Science & Technology, New York, 4 – 8 March 2013, accepted for publication in Nuclear Data Sheets, January 2014.

F. Mingrone, C. Massimi, G. Vannini and the n_TOF collaboration, "^{238}U(n,γ) reaction cross section measurement with C6D6 detectors at the n_TOF CERN facility", International Nuclear Physics Conference, Firenze, Italy 2 – 7 June 2013, to be published in European Physics Journal Web of Conferences

F. Mingrone, C. Massimi, G. Vannini and the n_TOF collaboration, "^{238}U(n,γ) reaction cross section measurement with C6D6 detectors at the n_TOF CERN facility", Proceedings of the 3rd European Energy Conference – E2C 2013, 27 – 30 October, 2013, Budapest, Hungary.

References

[1] Project within the Seventh Framework Program of the European Commission, "Accurate Nuclear Data for nuclear Energy Sustainability", ANDES (FP7-249671).

[2] M.B. Chadwick, E. Dupont et al., "The CIELO Collaboration: Neutron Reactions on ^{1}H, ^{16}O, ^{56}Fe, ^{235,238}U, and ^{239}Pu", accepted for publication in Nuclear Data Sheets (January 2014).

[3] OECD NEA High Priority Request List http://www.oecd-nea.org/dbdata/hprl/ (27/06/2013).

[4] C. Lampoudis, S. Kopecky, B. Becker, F. Gunsing, P. Schillebeeckx and R. Wynants, "^{238}U neutron capture cross section measurements in the unresolved resonance region at the GELINA facility", presented at the International Conference on Nuclear Data for Science & Technology, New York, 4 – 8 March 2013, accepted for publication in Nuclear Data Sheets, January 2014.

[5] F. Mingrone, C. Massimi, G. Vannini and the n_TOF collaboration, "Measurement of the ^{238}U radiative capture cross section with C_6D_6 at the CERN n_TOF facility", presented at the International Conference on Nuclear Data for Science & Technology, New York, 4 – 8 March 2013, accepted for publication in Nuclear Data Sheets, January 2014.

[6] T. Wright, C. Guerrero, J. Billowes, T. Ware, D. Cano-Ott, E. Mendoza and the n_TOF collaboration, "High-precision measurement of the ^{238}U(n,γ) cross section with the Total Absorption Calorimeter (TAC) at n_TOF, CERN", presented at the International Conference on Nuclear Data for Science & Technology, New York, 4 – 8 March 2013, accepted for publication in Nuclear Data Sheets, January 2014.

[7] P. Schillebeeckx, B. Becker, Y. Danon, K. Guber, H. Harada, J. Heyse, A.R. Junghans, S. Kopecky, C. Massimi, M.C. Moxon, N. Otuka, I. Sirakov and K. Volev, "Determination of resonance parameters and their covariances from neutron induced reaction cross section data", Nuclear Data Sheets 113 (2012) 3054 – 3100.

[8] A. Borella, G. Aerts, F. Gunsing, M. Moxon, P. Schillebeeckx and R. Wynants, "The use of C_6D_6 detectors for neutron induced capture cross-section measurements in the resonance region," Nucl. Instr. Meth. A 577, (2007) 626 – 640.

[9] U. Abbondanno et al. (the n_TOF collaboration), "New experimental validation of the pulse height weighting technique for capture cross-section measurements", Nucl. Instr. Meth. A 521, (2004) 454 – 467.

[10] C. Guerrero et al., "The n_TOF Total Absorption Calorimeter for neutron capture measurements at CERN", Nucl. Instrum. Meth. A 608 (2009) 424-433.

[11] C. Lampoudis, S. Kopecky, O. Bouland, F. Gunsing, G. Noguere, A.J.M.Plompen, C. Sage, P. Schillebeeckx and R. Wynants, "Neutron transmission and capture cross section measurements for ^{241}Am at the GELINA facility", Eur. Phys. J. Plus, 128 (2013) 86.

[12] W. Mondelaers and P. Schillebeeckx, "GELINA, a neutron time-of-flight facility for neutron data measurements", Notiziario Neutroni e Luce di Sincrotrone, 11 (2006) 19 – 25

[13] D. Tronc, J.M. Salomé and K.H. Böckhoff, "A new pulse compression system for intense relativistic electron beams", Nucl. Instr. Meth., 228 (1985) 217 – 227.

[14] A. Bensussan and J.M. Salomé, "GELINA: A modern accelerator for high resolution neutron time of flight experiments", Nucl. Instr. Meth., 155 (1978) 11 – 23.

[15] L. Mihailescu, A. Borella, C. Massimi and P. Schillebeeckx, "Investigations for the use of fast digitizers with C6D6 detectors for radiative capture measurements at GELINA", Nucl. Instr. Meth. A 600 (2009) 453 – 459.

[16] B. Becker, C. Bastian, F. Emiliani, F. Gunsing, J. Heyse, K. Kauwenberghs, S. Kopecky, C. Lampoudis, C. Massimi, N. Otuka, P. Schillebeeckx and I. Sirakov, "Data reduction and uncertainty propagation of time-of-flight spectra with AGS", J. of Instrumentation, 7 (2012) P11002 – 19.

[17] N. Otuka, A. Borella, S. Kopecky, C. Lampoudis, and P. Schillebeeckx, "Database for time-of-flight spectra with their covariances", J. Korean Phys. Soc. 59, (2011) 1314 – 1317.

[18] D.K. Olsen, G. de Saussure, R.B. Perez, E.G. Silver, F.C. Difilippo, R.W. Ingle, H. Weaver, "Precise Measurement and Analysis of Neutron Transmission Through Uranium-238" Nucl. Sci Eng. 62 (1977) 479 – 501.

[19] D.K. Olsen, G. de Saussure, R.B. Perez, F.C. Difilippo, R.W. Ingle, "Note on ^{238}U + n Resolved Resonance Energies", Nucl. Sci. Eng. 66 (1978) 141 –144.

[20] D.K. Olsen, G. de Saussure, R.B. Perez, F.C. Difilippo, R.W. Ingle, H. Weaver, "Measurement and Resonance Analysis of Neutron Transmission Through Uranium-238", Nucl. Sci. Eng. 69 (1979) 202 – 222.

[21] D.K. Olsen, P.S. Meszaros, "Resolved Resonance Parameters for ^{238}U from 4 to 6 keV", Nucl. Sci. Eng. 83 (1983) 174 – 181.

[22] D.K. Olsen, "Resolved Resonance Parameters for ^{238}U from 1 to 10 keV", Nucl. Sci. Eng. 94 (1986) 102 – 106.

[23] J.A. Harvey, N.W. Hill, F.G. Perey, G.L. Tweed, L. Leal, "High-Resolution Neutron Transmission Measurements on ^{235}U, ^{239}Pu, and ^{238}U", presented at the International Conference on Nuclear Data for Science & Technology, Mito, Japan, 30 May - 3 June, 1988, 115 – 118.

[24] A. Meister et al., "Experimental Study of the Doppler Broadening of Neutron Resonances at GELINA", International Conference on Nuclear Data for Science and Technology (NDST-97), Trieste, Italy, 19-24 May, 1997, 435 – 439.

[25] H. Derrien, L.C. Leal, N.M. Larson, A. Courcelle, "Neutron Resonance Parameters and Calculated Cross Sections from Reich-Moore Analysis of Experimental Data in the Neutron Energy Range from 0 to 20 keV", ORNL/TM-2005/241, Oak Ridge National Laboratory, (2005).

[26] K. Volev, A. Borella, S. Kopecky, C. Lampoudis, C. Massimi, A. Moens, M. Moxon,P. Schillebeeckx, P. Siegler, I. Sirakov, A. Trkov, R. Wynants, "Evaluation of resonance parameters for neutron induced reactions in cadmium", Nucl. Instr. Meth. B 300 (2013) 11 – 29.

[27] I. Sirakov, B. Becker, R. Capote, E. Dupont, S. Kopecky, C. Massimi, P. Schillebeeckx, "Results of total cross section measurements for ^{197}Au in the neutron energy region from 4 to 108 keV at GELINA", accepted for publication in Eur. Phys. J. A (2013).

[28] A. Borella, K. Volev, A. Brusegan, P. Schillebeeckx, F. Corvi, N. Koyumdjieva, N. Janeva, A.A. Lukyanov, "Determination of the ^{232}Th(n,γ) Cross Section from 4 to 140 keV at GELINA", Nucl. Sci Eng. 152 (2006) 1 – 14.

[29] A.D. Carlson, V.G. Pronyaev, D.L. Smith, N.M. Larson, Z. Chen, G.M. Hale, F.-J. Hambsch, E.V. Gai, Soo-Youl Oh, S.A. Badikov, T. Kawano, H.M. Hofman, H. Vonach, and S. Tagesen, "International evaluation of neutron cross section standards", Nuclear Data Sheets 110, (2009) 3215 – 3324.

[30] G. D'Agostini, "On the use of the covariance matrix to fit correlated data", Nucl. Instrum. Meth. A (1994) 306.

[31] B. Becker, R. Capote, S. Kopecky, C. Massimi, P. Schillebeeckx, I. Sirakov, K. Volev, "Evaluation of the covariance matrix of estimated resonance parameters", presented at the International Conference on Nuclear Data for Science & Technology, New York, 4 – 8 March 2013, accepted for publication in Nuclear Data Sheets, January 2014.

[32] M.C. Moxon, J.B. Brisland, "GEEL REFIT, A least squares fitting program for resonance analysis of neutron transmission and capture data computer code", AEAInTec-0630, AEA Technology, October (1991).

[33] C. W. Reich, M. S. Moore, "Multilevel formula for the fission process", Phys. Rev. 111 (1958) 929 – 933.

[34] P. Schillebeeckx, A. Borella, S. Kopecky, C. Lampoudis, C. Massimi and M. Moxon, "Neutron resonance spectroscopy at GELINA", J. Korean Phys. Soc. 59 (2011) 1563 –1568..

[35] B. Becker, S. Kopecky, H. Harada, P. Schillebeeckx, "Measurement of the particle self-shielding using neutron resonance transmission analysis", submitted to J. Quant. Spectrosc. Radiat. Transfer

[36] R. Dagan, B. Becker, Y. Danon, F. Gunsing, S. Kopecky, C. Lampoudis, O. Litaize, M. Moxon, P. Schillebeeckx, "Impact of the Doppler Broadened Double Differential Cross Section on Observed Resonance Profiles" presented at the International Conference on Nuclear Data for Science & Technology, New York, 4 – 8 March 2013, accepted for publication in Nuclear Data Sheets, January 2014.

[37] B. Becker, R. Dagan, G. Lohnert, "Proof and implementation of the stochastic formula for ideal gas, energy dependent scattering kernel", Ann. Nucl. Energy 36 (2009) 470 – 474.

[38] C. Guerrero et al., "Performance of the neutron time-of-flight facility n_TOF at CERN", Eur. Phys. J. **A** (2013) 49: 27.

[39] S. Marrone et al. (The n_TOF Collaboration), "A low background neutron flux monitor for the n_TOF facility at CERN", Nucl. Intrum. and Meth. A 517 (2004) 389 – 398.

[40] C. Massimi et al. (The n_TOF Collaboration), "^{197}Au(n,γ) cross section in the resonance region", Phys. Rev. C 81 (2010) 044616.

[41] E. Mendoza et al., "Improved Neutron Capture Cross Section Measurements with the n_TOF Total Absorption Calorimeter", J. Korean Phys. Soc. 59 (2011) 1813 – 1816.

[42] U. Abbondanno et al., "The data acquisition system of the neutron time-of-flight facility n_TOF at CERN", Nucl. Instr. And Meth. A 538 (2005) 692 – 702.

[43] R. Plag, M. Heil, F. Käppeler, P. Pavlopoulos, R. Reifarth, K. Wisshak, The n_TOF Collaboration, "An optimized C_6D_6 detector for studies of resonance-dominated (n,γ) cross-sections", Nucl. Instr. And Meth. A 496 (2003) 425 – 436.

[44] N.M. Larson, "Updated users guide for SAMMY: Multilevel R-matrix fits to neutron data using Bayes' equations", Report ORNL/TM-9179/R8 and ENDF-364/R2, Oak Ridge National Laboratory, USA, (2008).

[45] E. Mendoza, D. Cano-Ott, C. Guerrero, E. Berthoumieuz, "Pulse pile-up and dead-time correction methods applied to the digitised signals of a segmented BaF_2 Total Absorption Calorimeter used in (n,γ) cross section measurements", Nucl. Intrum. and Meth. A (in preparation).

[46] C. Guerrero, D. Cano-Ott and E. Mendoza, "A Monte Carlo based pile-up and dead-time correction method for measurements in coincidence with detector arrays", Nucl. Intrum. and Meth. A (in preparation).

European Commission
EUR 26478 EN – Joint Research Centre – Institute for Reference Materials and Measurements

Title: Total and radiative capture cross section measurements for ^{238}U at GELINA and n_TOF - Deliverable for the ANDES project

Authors: P. Schillebeeckx, C. Lampoudis, F. Mingrone, T. Wright, B. Becker, E. Berthoumieux, J. Billowes, D. Cano-Ott, R. Dagan, J.C. Drohe, C. Guerrero, F. Gunsing, S. Kopecky, C. Massimi, E. Mendoza, G. Vannini, R. Wynants and the n_TOF collaboration

Luxembourg: Publications Office of the European Union

2013 – 25 pp. – 21.0 x 29.7 cm

EUR – Scientific and Technical Research series – ISSN 1831-9424 (online)

ISBN 978-92-79-35279-9 (pdf)

doi:10.2787/86726

Abstract

This report comprises the deliverable D1.8 of the ANDES project (EURATOM contract FP7-249671) of Task 1.2 "High accuracy measurements of neutron capture cross sections" of Work Package 1. This deliverable provides evidence of a successful completion of subtasks 1.2.a and 1.2.c of Task 1.2.

The main objective of these subtasks was to obtain accurate capture cross section data (i.e. capture yields) from measurements at the time-of-flight facilities GELINA and n_TOF in response to the Nuclear Data High Priority Request List. The data produced within the ANDES project will be used to produce a new evaluation of the cross section for the neutron induced capture reaction on ^{238}U with an accuracy between 1% - 2% for neutron energies between 22 eV and 25 keV.

LA-NA-26478-EN-N

As the Commission's in-house science service, the Joint Research Centre's mission is to provide EU policies with independent, evidence-based scientific and technical support throughout the whole policy cycle.

Working in close cooperation with policy Directorates-General, the JRC addresses key societal challenges while stimulating innovation through developing new standards, methods and tools, and sharing and transferring its know-how to the Member States and international community.

Key policy areas include: environment and climate change; energy and transport; agriculture and food security; health and consumer protection; information society and digital agenda; safety and security including nuclear; all supported through a cross-cutting and multi-disciplinary approach.

ISBN 978-92-79-35279-9

Publications Office